

### 3 Quark masses

Quark masses are fundamental parameters of the Standard Model. An accurate determination of these parameters is important for both phenomenological and theoretical applications. The charm and bottom masses, for instance, enter the theoretical expressions of several cross sections and decay rates in heavy-quark expansions. The up-, down- and strange-quark masses govern the amount of explicit chiral symmetry breaking in QCD. From a theoretical point of view, the values of quark masses provide information about the flavour structure of physics beyond the Standard Model. The Review of Particle Physics of the Particle Data Group contains a review of quark masses [1], which covers light as well as heavy flavours. Here we also consider light- and heavy- quark masses, but focus on lattice results and discuss them in more detail. We do not discuss the top quark, however, because it decays weakly before it can hadronize, and the nonperturbative QCD dynamics described by present day lattice simulations is not relevant. The lattice determination of light- (up, down, strange), charm- and bottom-quark masses is considered below in Secs. 3.1, 3.2, and 3.3, respectively.

Quark masses cannot be measured directly in experiment because quarks cannot be isolated, as they are confined inside hadrons. On the other hand, quark masses are free parameters of the theory and, as such, cannot be obtained on the basis of purely theoretical considerations. Their values can only be determined by comparing the theoretical prediction for an observable, which depends on the quark mass of interest, with the corresponding experimental value.

In the last edition of this review [2], quark-mass determinations came from two- and three-flavour QCD calculations. Moreover, these calculations were most often performed in the isospin limit, where the up- and down-quark masses (especially those in the sea) are set equal. In addition, some of the results retained in our light-quark mass averages were based on simulations performed at values of  $m_{ud}$  which were still substantially larger than its physical value imposing a significant extrapolation to reach the physical up- and down-quark mass point. Among the calculations performed near physical  $m_{ud}$  by PACS-CS [3–5], BMW [6, 7] and RBC/UKQCD [8], only the ones in Refs. [6, 7] did so while controlling all other sources of systematic error.

Today, however, the effects of the charm quark in the sea are more and more systematically considered and most of the new quark-mass results discussed below have been obtained in  $N_f = 2 + 1 + 1$  simulations by ETM [9], HPQCD [10] and FNAL/MILC [11]. In addition, RBC/UKQCD [12], HPQCD [10] and FNAL/MILC [11] are extending their calculations down to up-down-quark masses at or very close to their physical values while still controlling other sources of systematic error. Another aspect that is being increasingly addressed are electromagnetic and  $(m_d - m_u)$ , strong isospin-breaking effects. As we will see below these are particularly important for determining the individual up- and down-quark masses. But with the level of precision being reached in calculations, these effects are also becoming important for other quark masses.

Three-flavour QCD has four free parameters: the strong coupling,  $\alpha_s$  (alternatively  $\Lambda_{\text{QCD}}$ ) and the up-, down- and strange-quark masses,  $m_u$ ,  $m_d$  and  $m_s$ . Four-flavour calculations have an additional parameter, the charm-quark mass  $m_c$ . When the calculations are performed in the isospin limit, up- and down-quark masses are replaced by a single parameter: the isospin-averaged up- and down-quark mass,  $m_{ud} = \frac{1}{2}(m_u + m_d)$ . A lattice determination of these parameters, and in particular of the quark masses, proceeds in two steps:

1. One computes as many experimentally measurable quantities as there are quark masses. These observables should obviously be sensitive to the masses of interest, preferably straightforward to compute and obtainable with high precision. They are usually computed for a variety of input values of the quark masses which are then adjusted to reproduce experiment. Another observable, such as the pion decay constant or the mass of a member of the baryon octet, must be used to fix the overall scale. Note that the mass of a quark, such as the  $b$ , which is not accounted for in the generation of gauge configurations, can still be determined. For that an additional valence-quark observable containing this quark must be computed and the mass of that quark must be tuned to reproduce experiment.
2. The input quark masses are bare parameters which depend on the lattice spacing and particulars of the lattice regularization used in the calculation. To compare their values at different lattice spacings and to allow a continuum extrapolation they must be renormalized. This renormalization is a short-distance calculation, which may be performed perturbatively. Experience shows that 1-loop calculations are unreliable for the renormalization of quark masses: usually at least two loops are required to have trustworthy results. Therefore, it is best to perform the renormalizations nonperturbatively to avoid potentially large perturbative uncertainties due to neglected higher-order terms. Nevertheless we will include in our averages 1-loop results if they carry a solid estimate of the systematic uncertainty due to the truncation of the series.

In the absence of electromagnetic corrections, the renormalization factors for all quark masses are the same at a given lattice spacing. Thus, uncertainties due to renormalization are absent in ratios of quark masses if the tuning of the masses to their physical values can be done lattice spacing by lattice spacing and significantly reduced otherwise.

We mention that lattice QCD calculations of the  $b$ -quark mass have an additional complication which is not present in the case of the charm- and light-quarks. At the lattice spacings currently used in numerical simulations the direct treatment of the  $b$  quark with the fermionic actions commonly used for light quarks will result in large cutoff effects, because the  $b$ -quark mass is of order one in lattice units. There are a few widely used approaches to treat the  $b$  quark on the lattice, which have been already discussed in the FLAG 13 review (see Section 8 of Ref. [2]). Those relevant for the determination of the  $b$ -quark mass will be briefly described in Sec. 3.3.

### 3.1 Masses of the light quarks

Light-quark masses are particularly difficult to determine because they are very small (for the up and down quarks) or small (for the strange quark) compared to typical hadronic scales. Thus, their impact on typical hadronic observables is minute, and it is difficult to isolate their contribution accurately.

Fortunately, the spontaneous breaking of  $SU(3)_L \times SU(3)_R$  chiral symmetry provides observables which are particularly sensitive to the light-quark masses: the masses of the resulting Nambu-Goldstone bosons (NGB), i.e. pions, kaons and etas. Indeed, the Gell-Mann-Oakes-Renner relation [13] predicts that the squared mass of a NGB is directly proportional to the sum of the masses of the quark and antiquark which compose it, up to higher-order mass corrections. Moreover, because these NGBs are light and are composed of only two valence particles, their masses have a particularly clean statistical signal in lattice-QCD calculations.

In addition, the experimental uncertainties on these meson masses are negligible. Thus, in lattice calculations, light-quark masses are typically obtained by renormalizing the input quark mass and tuning them to reproduce NGB masses, as described above.

### 3.1.1 Contributions from the electromagnetic interaction

As mentioned in Sec. 2.1, the present review relies on the hypothesis that, at low energies, the Lagrangian  $\mathcal{L}_{\text{QCD}} + \mathcal{L}_{\text{QED}}$  describes nature to a high degree of precision. However, most of the results presented below are obtained in pure QCD calculations, which do not include QED. Quite generally, when comparing QCD calculations with experiment, radiative corrections need to be applied. In pure QCD simulations, where the parameters are fixed in terms of the masses of some of the hadrons, the electromagnetic contributions to these masses must be accounted for. Of course, once QED is included in lattice calculations, the subtraction of e.m. contributions is no longer necessary.

The electromagnetic interaction plays a particularly important role in determinations of the ratio  $m_u/m_d$ , because the isospin-breaking effects generated by this interaction are comparable to those from  $m_u \neq m_d$  (see Subsection 3.1.5). In determinations of the ratio  $m_s/m_{ud}$ , the electromagnetic interaction is less important, but at the accuracy reached, it cannot be neglected. The reason is that, in the determination of this ratio, the pion mass enters as an input parameter. Because  $M_\pi$  represents a small symmetry-breaking effect, it is rather sensitive to the perturbations generated by QED.

The decomposition of the sum  $\mathcal{L}_{\text{QCD}} + \mathcal{L}_{\text{QED}}$  into two parts is not unique and specifying the QCD part requires a convention. In order to give results for the quark masses in the Standard Model at scale  $\mu = 2\text{ GeV}$ , on the basis of a calculation done within QCD, it is convenient to match the parameters of the two theories at that scale. We use this convention throughout the present review.<sup>1</sup>

Such a convention allows us to distinguish the physical mass  $M_P$ ,  $P \in \{\pi^+, \pi^0, K^+, K^0\}$ , from the mass  $\hat{M}_P$  within QCD. The e.m. self-energy is the difference between the two,  $M_P^\gamma \equiv M_P - \hat{M}_P$ . Because the self-energy of the Nambu-Goldstone bosons diverges in the chiral limit, it is convenient to replace it by the contribution of the e.m. interaction to the *square* of the mass,

$$\Delta_P^\gamma \equiv M_P^2 - \hat{M}_P^2 = 2 M_P M_P^\gamma + \mathcal{O}(e^4). \quad (9)$$

The main effect of the e.m. interaction is an increase in the mass of the charged particles, generated by the photon cloud that surrounds them. The self-energies of the neutral ones are comparatively small, particularly for the Nambu-Goldstone bosons, which do not have a magnetic moment. Dashen's theorem [19] confirms this picture, as it states that, to leading order (LO) of the chiral expansion, the self-energies of the neutral NGBs vanish, while the charged ones obey  $\Delta_{K^+}^\gamma = \Delta_{\pi^+}^\gamma$ . It is convenient to express the self-energies of the neutral particles as well as the mass difference between the charged and neutral pions within QCD in units of the observed mass difference,  $\Delta_\pi \equiv M_{\pi^+}^2 - M_{\pi^0}^2$ :

$$\Delta_{\pi^0}^\gamma \equiv \epsilon_{\pi^0} \Delta_\pi, \quad \Delta_{K^0}^\gamma \equiv \epsilon_{K^0} \Delta_\pi, \quad \hat{M}_{\pi^+}^2 - \hat{M}_{\pi^0}^2 \equiv \epsilon_m \Delta_\pi. \quad (10)$$

<sup>1</sup>Note that a different convention is used in the analysis of the precision measurements carried out in low-energy pion physics (e.g. Ref. [14]). When comparing lattice results with experiment, it is important to fix the QCD parameters in accordance with the convention used in the analysis of the experimental data (for a more detailed discussion, see Refs. [15–18]).

In this notation, the self-energies of the charged particles are given by

$$\Delta_{\pi^+}^\gamma = (1 + \epsilon_{\pi^0} - \epsilon_m) \Delta_\pi, \quad \Delta_{K^+}^\gamma = (1 + \epsilon + \epsilon_{K^0} - \epsilon_m) \Delta_\pi, \quad (11)$$

where the dimensionless coefficient  $\epsilon$  parameterizes the violation of Dashen's theorem,<sup>2</sup>

$$\Delta_{K^+}^\gamma - \Delta_{K^0}^\gamma - \Delta_{\pi^+}^\gamma + \Delta_{\pi^0}^\gamma \equiv \epsilon \Delta_\pi. \quad (12)$$

Any determination of the light-quark masses based on a calculation of the masses of  $\pi^+$ ,  $K^+$  and  $K^0$  within QCD requires an estimate for the coefficients  $\epsilon$ ,  $\epsilon_{\pi^0}$ ,  $\epsilon_{K^0}$  and  $\epsilon_m$ .

The first determination of the self-energies on the lattice was carried out by Duncan, Eichten and Thacker [21]. Using the quenched approximation, they arrived at  $M_{K^+}^\gamma - M_{K^0}^\gamma = 1.9$  MeV. Actually, the parameterization of the masses given in that paper yields an estimate for all but one of the coefficients introduced above (since the mass splitting between the charged and neutral pions in QCD is neglected, the parameterization amounts to setting  $\epsilon_m = 0$  ab initio). Evaluating the differences between the masses obtained at the physical value of the electromagnetic coupling constant and at  $e = 0$ , we obtain  $\epsilon = 0.50(8)$ ,  $\epsilon_{\pi^0} = 0.034(5)$  and  $\epsilon_{K^0} = 0.23(3)$ . The errors quoted are statistical only: an estimate of lattice systematic errors is not possible from the limited results of Ref. [21]. The result for  $\epsilon$  indicates that the violation of Dashen's theorem is sizeable: according to this calculation, the nonleading contributions to the self-energy difference of the kaons amount to 50% of the leading term. The result for the self-energy of the neutral pion cannot be taken at face value, because it is small, comparable to the neglected mass difference  $\hat{M}_{\pi^+} - \hat{M}_{\pi^0}$ . To illustrate this, we note that the numbers quoted above are obtained by matching the parameterization with the physical masses for  $\pi^0$ ,  $K^+$  and  $K^0$ . This gives a mass for the charged pion that is too high by 0.32 MeV. Tuning the parameters instead such that  $M_{\pi^+}$  comes out correctly, the result for the self-energy of the neutral pion becomes larger:  $\epsilon_{\pi^0} = 0.10(7)$  where, again, the error is statistical only.

In an update of this calculation by the RBC collaboration [22] (RBC 07), the electromagnetic interaction is still treated in the quenched approximation, but the strong interaction is simulated with  $N_f = 2$  dynamical quark flavours. The quark masses are fixed with the physical masses of  $\pi^0$ ,  $K^+$  and  $K^0$ . The outcome for the difference in the electromagnetic self-energy of the kaons reads  $M_{K^+}^\gamma - M_{K^0}^\gamma = 1.443(55)$  MeV. This corresponds to a remarkably small violation of Dashen's theorem. Indeed, a recent extension of this work to  $N_f = 2 + 1$  dynamical flavours [20] leads to a significantly larger self-energy difference:  $M_{K^+}^\gamma - M_{K^0}^\gamma = 1.87(10)$  MeV, in good agreement with the estimate of Eichten et al. Expressed in terms of the coefficient  $\epsilon$  that measures the size of the violation of Dashen's theorem, it corresponds to  $\epsilon = 0.5(1)$ .

The input for the electromagnetic corrections used by MILC is specified in Ref. [23]. In their analysis of the lattice data,  $\epsilon_{\pi^0}$ ,  $\epsilon_{K^0}$  and  $\epsilon_m$  are set equal to zero. For the remaining coefficient, which plays a crucial role in determinations of the ratio  $m_u/m_d$ , the very conservative range  $\epsilon = 1(1)$  was used in MILC 04 [24], while in MILC 09 [25] and MILC 09A [26] this input has been replaced by  $\epsilon = 1.2(5)$ , as suggested by phenomenological estimates for the corrections to Dashen's theorem [27, 28]. Results of an evaluation of the electromagnetic self-energies based on  $N_f = 2 + 1$  dynamical quarks in the QCD sector and on the quenched approximation in the QED sector have been also reported by MILC in Refs. [29–31] and

<sup>2</sup>Sometimes, e.g. in Ref. [20], the violation of Dashen's theorem is given in terms of a different quantity,  $\bar{\epsilon} \equiv (\Delta_{K^+}^\gamma - \Delta_{K^0}^\gamma)/(\Delta_{\pi^+}^\gamma - \Delta_{\pi^0}^\gamma) - 1$ . This parameter is related to  $\epsilon$  used here through  $\epsilon = (1 - \epsilon_m)\bar{\epsilon}$ . Given the value of  $\epsilon_m$  (see Eq. (13)), these two quantities differ by 4% only.

updated recently in Refs. [32, 33]. Their latest (preliminary) result is  $\bar{\epsilon} = 0.84(5)(19)$ , where the first error is statistical and the second systematic, coming from discretization and finite-volume uncertainties added in quadrature. With the estimate for  $\epsilon_m$  given in Eq. (13), this result corresponds to  $\epsilon = 0.81(5)(18)$ .

Preliminary results have been also reported by the BMW collaboration in conference proceedings [34–36], with the updated result being  $\epsilon = 0.57(6)(6)$ , where the first error is statistical and the second systematic.

The RM123 collaboration employs a new technique to compute e.m. shifts in hadron masses in 2-flavour QCD: the effects are included at leading order in the electromagnetic coupling  $\alpha$  through simple insertions of the fundamental electromagnetic interaction in quark lines of relevant Feynman graphs [37]. They find  $\epsilon = 0.79(18)(18)$ , where the first error is statistical and the second is the total systematic error resulting from chiral, finite-volume, discretization, quenching and fitting errors all added in quadrature.

Recently [38] the QCDSF/UKQCD collaboration has presented results for several pseudoscalar meson masses obtained from  $N_f = 2 + 1$  dynamical simulations of QCD + QED (at a single lattice spacing  $a \simeq 0.07$  fm). Using the experimental values of the  $\pi^0$ ,  $K^0$  and  $K^+$  mesons masses to fix the three light-quark masses, they find  $\epsilon = 0.50(6)$ , where the error is statistical only.

The effective Lagrangian that governs the self-energies to next-to-leading order (NLO) of the chiral expansion was set up in Ref. [39]. The estimates made in Refs. [27, 28] are obtained by replacing QCD with a model, matching this model with the effective theory and assuming that the effective coupling constants obtained in this way represent a decent approximation to those of QCD. For alternative model estimates and a detailed discussion of the problems encountered in models based on saturation by resonances, see Refs. [40–42]. In the present review of the information obtained on the lattice, we avoid the use of models altogether.

There is an indirect phenomenological determination of  $\epsilon$ , which is based on the decay  $\eta \rightarrow 3\pi$  and does not rely on models. The result for the quark-mass ratio  $Q$ , defined in Eq. (32) and obtained from a dispersive analysis of this decay, implies  $\epsilon = 0.70(28)$  (see Sec. 3.1.5). While the values found in older lattice calculations [20–22] are a little less than one standard deviation lower, the most recent determinations [29–35, 37, 43], though still preliminary, are in excellent agreement with this result and have significantly smaller error bars. However, even in the more recent calculations, e.m. effects are treated in the quenched approximation. Thus, we choose to quote  $\epsilon = 0.7(3)$ , which is essentially the  $\eta \rightarrow 3\pi$  result and covers the range of post-2010 lattice results. Note that this value has an uncertainty which is reduced by about 40% compared to the result quoted in the first edition of the FLAG review [44].

We add a few comments concerning the physics of the self-energies and then specify the estimates used as an input in our analysis of the data. The Cottingham formula [45] represents the self-energy of a particle as an integral over electron scattering cross sections; elastic as well as inelastic reactions contribute. For the charged pion, the term due to elastic scattering, which involves the square of the e.m. form factor, makes a substantial contribution. In the case of the  $\pi^0$ , this term is absent, because the form factor vanishes on account of charge conjugation invariance. Indeed, the contribution from the form factor to the self-energy of the  $\pi^+$  roughly reproduces the observed mass difference between the two particles. Furthermore, the numbers given in Refs. [46–48] indicate that the inelastic contributions are significantly smaller than the elastic contributions to the self-energy of the  $\pi^+$ . The low-energy theorem of Das, Guralnik, Mathur, Low and Young [49] ensures that, in the limit  $m_u, m_d \rightarrow 0$ , the e.m. self-energy of the  $\pi^0$  vanishes, while the one of the  $\pi^+$  is given by an integral over

the difference between the vector and axial-vector spectral functions. The estimates for  $\epsilon_{\pi^0}$  obtained in Ref. [21] and more recently in Ref. [38] are consistent with the suppression of the self-energy of the  $\pi^0$  implied by chiral  $SU(2) \times SU(2)$ . In our opinion, as already done in the FLAG 13 review [2], the value  $\epsilon_{\pi^0} = 0.07(7)$  still represents a quite conservative estimate for this coefficient. The self-energy of the  $K^0$  is suppressed less strongly, because it remains different from zero if  $m_u$  and  $m_d$  are taken massless and only disappears if  $m_s$  is turned off as well. Note also that, since the e.m. form factor of the  $K^0$  is different from zero, the self-energy of the  $K^0$  does pick up an elastic contribution. The recent lattice result  $\epsilon_{K^0} = 0.2(1)$  obtained in Ref. [38] indicates that the violation of Dashen's theorem is smaller than in the case of  $\epsilon$ . Following the FLAG 13 review [2] we confirm the choice of the conservative value  $\epsilon_{K^0} = 0.3(3)$ .

Finally, we consider the mass splitting between the charged and neutral pions in QCD. This effect is known to be very small, because it is of second order in  $m_u - m_d$ . There is a parameter-free prediction, which expresses the difference  $\hat{M}_{\pi^+}^2 - \hat{M}_{\pi^0}^2$  in terms of the physical masses of the pseudoscalar octet and is valid to NLO of the chiral perturbation series. Numerically, the relation yields  $\epsilon_m = 0.04$  [50], indicating that this contribution does not play a significant role at the present level of accuracy. We attach a conservative error also to this coefficient:  $\epsilon_m = 0.04(2)$ . The lattice result for the self-energy difference of the pions, reported in Ref. [20],  $M_{\pi^+}^\gamma - M_{\pi^0}^\gamma = 4.50(23)$  MeV, agrees with this estimate: expressed in terms of the coefficient  $\epsilon_m$  that measures the pion-mass splitting in QCD, the result corresponds to  $\epsilon_m = 0.04(5)$ . The corrections of next-to-next-to-leading order (NNLO) have been worked out in Ref. [51], but the numerical evaluation of the formulae again meets with the problem that the relevant effective coupling constants are not reliably known.

In summary, we use the following estimates for the e.m. corrections:

$$\epsilon = 0.7(3), \quad \epsilon_{\pi^0} = 0.07(7), \quad \epsilon_{K^0} = 0.3(3), \quad \epsilon_m = 0.04(2). \quad (13)$$

While the range used for the coefficient  $\epsilon$  affects our analysis in a significant way, the numerical values of the other coefficients only serve to set the scale of these contributions. The range given for  $\epsilon_{\pi^0}$  and  $\epsilon_{K^0}$  may be overly generous, but because of the exploratory nature of the lattice determinations, we consider it advisable to use a conservative estimate.

Treating the uncertainties in the four coefficients as statistically independent and adding errors in quadrature, the numbers in Eq. (13) yield the following estimates for the e.m. self-energies,

$$\begin{aligned} M_{\pi^+}^\gamma &= 4.7(3) \text{ MeV}, & M_{\pi^0}^\gamma &= 0.3(3) \text{ MeV}, & M_{\pi^+}^\gamma - M_{\pi^0}^\gamma &= 4.4(1) \text{ MeV}, \\ M_{K^+}^\gamma &= 2.5(5) \text{ MeV}, & M_{K^0}^\gamma &= 0.4(4) \text{ MeV}, & M_{K^+}^\gamma - M_{K^0}^\gamma &= 2.1(4) \text{ MeV}, \end{aligned} \quad (14)$$

and for the pion and kaon masses occurring in the QCD sector of the Standard Model,

$$\begin{aligned} \hat{M}_{\pi^+} &= 134.8(3) \text{ MeV}, & \hat{M}_{\pi^0} &= 134.6(3) \text{ MeV}, & \hat{M}_{\pi^+} - \hat{M}_{\pi^0} &= 0.2(1) \text{ MeV}, \\ \hat{M}_{K^+} &= 491.2(5) \text{ MeV}, & \hat{M}_{K^0} &= 497.2(4) \text{ MeV}, & \hat{M}_{K^+} - \hat{M}_{K^0} &= -6.1(4) \text{ MeV}. \end{aligned} \quad (15)$$

The self-energy difference between the charged and neutral pion involves the same coefficient  $\epsilon_m$  that describes the mass difference in QCD – this is why the estimate for  $M_{\pi^+}^\gamma - M_{\pi^0}^\gamma$  is so precise.

### 3.1.2 Pion and kaon masses in the isospin limit

As mentioned above, most of the lattice calculations concerning the properties of the light mesons are performed in the isospin limit of QCD ( $m_u - m_d \rightarrow 0$  at fixed  $m_u + m_d$ ). We denote the pion and kaon masses in that limit by  $\bar{M}_\pi$  and  $\bar{M}_K$ , respectively. Their numerical values can be estimated as follows. Since the operation  $u \leftrightarrow d$  interchanges  $\pi^+$  with  $\pi^-$  and  $K^+$  with  $K^0$ , the expansion of the quantities  $\hat{M}_{\pi^+}^2$  and  $\frac{1}{2}(\hat{M}_{K^+}^2 + \hat{M}_{K^0}^2)$  in powers of  $m_u - m_d$  only contains even powers. As shown in Ref. [52], the effects generated by  $m_u - m_d$  in the mass of the charged pion are strongly suppressed: the difference  $\hat{M}_{\pi^+}^2 - \bar{M}_\pi^2$  represents a quantity of  $\mathcal{O}[(m_u - m_d)^2(m_u + m_d)]$  and is therefore small compared to the difference  $\hat{M}_{\pi^+}^2 - \hat{M}_{\pi^0}^2$ , for which an estimate was given above. In the case of  $\frac{1}{2}(\hat{M}_{K^+}^2 + \hat{M}_{K^0}^2) - \bar{M}_K^2$ , the expansion does contain a contribution at NLO, determined by the combination  $2L_8 - L_5$  of low-energy constants, but the lattice results for that combination show that this contribution is very small, too. Numerically, the effects generated by  $m_u - m_d$  in  $\hat{M}_{\pi^+}^2$  and in  $\frac{1}{2}(\hat{M}_{K^+}^2 + \hat{M}_{K^0}^2)$  are negligible compared to the uncertainties in the electromagnetic self-energies. The estimates for these given in Eq. (15) thus imply

$$\bar{M}_\pi = \hat{M}_{\pi^+} = 134.8(3) \text{ MeV} , \quad \bar{M}_K = \sqrt{\frac{1}{2}(\hat{M}_{K^+}^2 + \hat{M}_{K^0}^2)} = 494.2(3) \text{ MeV} . \quad (16)$$

This shows that, for the convention used above to specify the QCD sector of the Standard Model, and within the accuracy to which this convention can currently be implemented, the mass of the pion in the isospin limit agrees with the physical mass of the neutral pion:  $\bar{M}_\pi - M_{\pi^0} = -0.2(3) \text{ MeV}$ .

### 3.1.3 Lattice determination of $m_s$ and $m_{ud}$

We now turn to a review of the lattice calculations of the light-quark masses and begin with  $m_s$ , the isospin-averaged up- and down-quark mass,  $m_{ud}$ , and their ratio. Most groups quote only  $m_{ud}$ , not the individual up- and down-quark masses. We then discuss the ratio  $m_u/m_d$  and the individual determination of  $m_u$  and  $m_d$ .

Quark masses have been calculated on the lattice since the mid-nineties. However early calculations were performed in the quenched approximation, leading to unquantifiable systematics. Thus in the following, we only review modern, unquenched calculations, which include the effects of light sea quarks.

Tabs. 3, 4 and 5 list the results of  $N_f = 2$ ,  $N_f = 2 + 1$  and  $N_f = 2 + 1 + 1$  lattice calculations of  $m_s$  and  $m_{ud}$ . These results are given in the  $\overline{\text{MS}}$  scheme at 2 GeV, which is standard nowadays, though some groups are starting to quote results at higher scales (e.g. Ref. [8]). The tables also show the colour coding of the calculations leading to these results. As indicated earlier in this review, we treat calculations with different numbers,  $N_f$ , of dynamical quarks separately.

#### *$N_f = 2$ lattice calculations*

For  $N_f = 2$ , no new calculations have been performed since the previous edition of the FLAG review [2]. A quick inspection of Tab. 3 indicates that only the more recent calculations, ALPHA 12 [53] and ETM 10B [54], control all systematic effects – the special case of Dürren 11 [55] is discussed below. Only ALPHA 12 [53], ETM 10B [54] and ETM 07 [56] really

enter the chiral regime, with pion masses down to about 270 MeV for ALPHA and ETM. Because this pion mass is still quite far from the physical pion mass, ALPHA 12 refrain from determining  $m_{ud}$  and give only  $m_s$ . All the other calculations have significantly more massive pions, the lightest being about 430 MeV, in the calculation by CP-PACS 01 [57]. Moreover, the latter calculation is performed on very coarse lattices, with lattice spacings  $a \geq 0.11$  fm and only 1-loop perturbation theory is used to renormalize the results.

ETM 10B's [54] calculation of  $m_{ud}$  and  $m_s$  is an update of the earlier twisted mass determination of ETM 07 [56]. In particular, they have added ensembles with a larger volume and three new lattice spacings,  $a = 0.054, 0.067$  and  $0.098$  fm, allowing for a continuum extrapolation. In addition, it features analyses performed in  $SU(2)$  and  $SU(3)$   $\chi$ PT.

The ALPHA 12 [53] calculation of  $m_s$  is an update of ALPHA 05 [58], which pushes computations to finer lattices and much lighter pion masses. It also importantly includes a determination of the lattice spacing with the decay constant  $F_K$ , whereas ALPHA 05 converted results to physical units using the scale parameter  $r_0$  [59], defined via the force between static quarks. In particular, the conversion relied on measurements of  $r_0/a$  by QCDSF/UKQCD 04 [60] which differ significantly from the new determination by ALPHA 12. As in ALPHA 05, in ALPHA 12 both nonperturbative running and nonperturbative renormalization are performed in a controlled fashion, using Schrödinger functional methods.

The conclusion of our analysis of  $N_f = 2$  calculations is that the results of ALPHA 12 [53] and ETM 10B [54] (which update and extend ALPHA 05 [58] and ETM 07 [56], respectively), are the only ones to date which satisfy our selection criteria. Thus we average those two results for  $m_s$ , obtaining 101(3) MeV. Regarding  $m_{ud}$ , for which only ETM 10B [54] gives a value, we do not offer an average but simply quote ETM's number. Thus, we quote as our estimates:

$$N_f = 2 : \quad \begin{array}{ll} m_s = 101(3) \text{ MeV} & \text{Refs. [53, 54],} \\ m_{ud} = 3.6(2) \text{ MeV} & \text{Ref. [54].} \end{array} \quad (17)$$

The errors on these results are 3% and 6%, respectively. However, these errors do not account for the fact that sea strange-quark mass effects are absent from the calculation, a truncation of the theory whose systematic effects cannot be estimated *a priori*. Thus, these results carry an additional unknown systematic error. It is worth remarking that the difference between ALPHA 12's [53] central value for  $m_s$  and that of ETM 10B [54] is 7(7) MeV.

We have not included the results of Dürr 11 [55] in the averages of Eq. (17), despite the fact that they satisfy our selection criteria. The reason for this is that the observable which they actually compute on the lattice is  $m_c/m_s = 11.27(30)(26)$ , reviewed in Sec. 3.2.4. They obtain  $m_s$  by combining that value of  $m_c/m_s$  with already existing phenomenological calculations of  $m_c$ . Subsequently they obtain  $m_{ud}$  by combining this result for  $m_s$  with the  $N_f = 2 + 1$  calculation of  $m_s/m_{ud}$  of BMW 10A, 10B [6, 7] discussed below. Thus, their results for  $m_s$  and  $m_{ud}$  are not *per se* lattice results, nor do they correspond to  $N_f = 2$ . The value of the charm-quark mass which they use is an average of phenomenological determinations, which they estimate to be  $m_c(2 \text{ GeV}) = 1.093(13) \text{ GeV}$ , with a 1.2% total uncertainty. This value for  $m_c$  leads to the results for  $m_s$  and  $m_{ud}$  in Tab. 3 which are compatible with the averages given in Eq. (17) and have similar uncertainties. Note, however, that their determination of  $m_c/m_s$  is about 1.5 combined standard deviations below the only other  $N_f = 2$  result which satisfies our selection criteria, ETM 10B's [54] result, as discussed in Sec. 3.2.4.



Collaboration	Ref.	publication status	chiral extrapolation	continuum extrapolation	finite volume	renormalization	running	$m_{ud}$	$m_s$
ALPHA 12	[53]	A	○	★	★	★	<i>a, b</i>		102(3)(1)
Dürr 11 <sup>‡</sup>	[55]	A	○	★	○	–	–	3.52(10)(9)	97.0(2.6)(2.5)
ETM 10B	[54]	A	○	★	○	★	<i>c</i>	3.6(1)(2)	95(2)(6)
JLQCD/TWQCD 08A	[61]	A	○	■	■	★	–	4.452(81)(38)( <sup>+0</sup> <sub>-227</sub> )	–
RBC 07 <sup>†</sup>	[22]	A	■	■	★	★	–	4.25(23)(26)	119.5(5.6)(7.4)
ETM 07	[56]	A	○	■	○	★	–	3.85(12)(40)	105(3)(9)
QCDSF/ UKQCD 06	[62]	A	■	★	■	★	–	4.08(23)(19)(23)	111(6)(4)(6)
SPQcdR 05	[63]	A	■	○	○	★	–	4.3(4)( <sup>+1.1</sup> <sub>-0.0</sub> )	101(8)( <sup>+25</sup> <sub>-0</sub> )
ALPHA 05	[58]	A	■	○	★	★	<i>a</i>		97(4)(18) <sup>§</sup>
QCDSF/ UKQCD 04	[60]	A	■	★	■	★	–	4.7(2)(3)	119(5)(8)
JLQCD 02	[64]	A	■	■	○	■	–	3.223( <sup>+46</sup> <sub>-69</sub> )	84.5( <sup>+12.0</sup> <sub>-1.7</sub> )
CP-PACS 01	[57]	A	■	■	★	■	–	3.45(10)( <sup>+11</sup> <sub>-18</sub> )	89(2)( <sup>+2</sup> <sub>-6</sub> ) <sup>*</sup>

<sup>‡</sup> What is calculated is  $m_c/m_s = 11.27(30)(26)$ .  $m_s$  is then obtained using lattice and phenomenological determinations of  $m_c$  which rely on perturbation theory. Finally,  $m_{ud}$  is determined from  $m_s$  using BMW 10A, 10B’s  $N_f = 2 + 1$  result for  $m_s/m_{ud}$  [6, 7]. Since  $m_c/m_s$  is renormalization group invariant in QCD, the renormalization and running of the quark masses enter indirectly through that of  $m_c$ , a mass that we do not review here.

<sup>†</sup> The calculation includes quenched e.m. effects.

<sup>§</sup> The data used to obtain the bare value of  $m_s$  are from UKQCD/QCDSF 04 [60].

<sup>\*</sup> This value of  $m_s$  was obtained using the kaon mass as input. If the  $\phi$ -meson mass is used instead, the authors find  $m_s = 90(<sup>+5</sup><sub>-11</sub>)$ .

*a* The masses are renormalized and run nonperturbatively up to a scale of 100 GeV in the  $N_f = 2$  SF scheme. In this scheme, nonperturbative and NLO running for the quark masses are shown to agree well from 100 GeV all the way down to 2 GeV [58].

*b* The running and renormalization results of Ref. [58] are improved in Ref. [53] with higher statistical and systematic accuracy.

*c* The masses are renormalized nonperturbatively at scales  $1/a \sim 2 \div 3$  GeV in the  $N_f = 2$  RI/MOM scheme. In this scheme, nonperturbative and N<sup>3</sup>LO running for the quark masses are shown to agree from 4 GeV down to 2 GeV to better than 3% [65].

Table 3:  $N_f = 2$  lattice results for the masses  $m_{ud}$  and  $m_s$  (MeV, running masses in the  $\overline{\text{MS}}$  scheme at scale 2 GeV). The significance of the colours is explained in Sec. 2. If information about nonperturbative running is available, this is indicated in the column “running”, with details given at the bottom of the table.

$N_f = 2 + 1$  lattice calculations

We turn now to  $N_f = 2 + 1$  calculations. These and the corresponding results for  $m_{ud}$  and  $m_s$  are summarized in Tab. 4. Given the very high precision of a number of the results, with total errors on the order of 1%, it is important to consider the effects neglected in these calculations. Since isospin breaking and e.m. effects are small on  $m_{ud}$  and  $m_s$ , and have been approximately accounted for in the calculations that will be retained for our averages, the largest potential source of uncontrolled systematic error is that due to the omission of the charm quark in the sea. Beyond the small perturbative corrections that come from matching the  $N_f = 3$  to the  $N_f = 4$   $\overline{\text{MS}}$  scheme at  $m_c$  ( $\sim -0.2\%$ ), the charm sea-quarks affect the determination of the light-quark masses through contributions of order  $1/m_c^2$ . As these are further suppressed by the Okubo-Zweig-Iizuka rule, they are also expected to be small, but are difficult to quantify *a priori*. Fortunately, as we will see below,  $m_s$  has been directly computed with  $N_f = 2+1+1$  simulations. In particular, HPQCD 14 [11] has computed  $m_s$  in QCD<sub>4</sub> with very much the same approach as it had used to obtain the QCD<sub>3</sub> result of HPQCD 10 [66]. Their results for  $m_s(N_f = 3, 2 \text{ GeV})$  are 93.8(8) MeV [11] and 92.2(1.3) MeV [66], where the  $N_f = 4$  result has been converted perturbatively to  $N_f = 3$  in Ref. [11]. This leads to a relative difference of 1.7(1.6)%. While the two results are compatible within one combined standard deviation, a  $\sim 2\%$  effect cannot be excluded. Thus, we will retain this 2% uncertainty and add it to the averages for  $m_s$  and  $m_{ud}$  given below.

The only new calculation since the last FLAG report [2] is that of RBC/UKQCD 14 [12]. It significantly improves on their RBC/UKQCD 12 [8] work by adding three new domain wall fermion simulations to three used previously. Two of the new simulations are performed at essentially physical pion masses ( $M_\pi \simeq 139 \text{ MeV}$ ) on lattices of about 5.4 fm in size and with lattice spacings of 0.114 fm and 0.084 fm. It is complemented by a third simulation with  $M_\pi \simeq 371 \text{ MeV}$ ,  $a \simeq 0.063$  and a rather small  $L \simeq 2.0 \text{ fm}$ . Altogether, this gives them six simulations with six unitary  $M_\pi$ 's in the range of 139 to 371 MeV and effectively three lattice spacings from 0.063 to 0.114 fm. They perform a combined global continuum and chiral fit to all of their results for the  $\pi$  and  $K$  masses and decay constants, the  $\Omega$  baryon mass and two Wilson-flow parameters. Quark masses in these fits are renormalized and run nonperturbatively in the RI/SMOM scheme. This is done by computing the relevant renormalization constant for a reference ensemble and determining those for other simulations relative to it by adding appropriate parameters in the global fit. This new calculation passes all of our selection criteria. Its results will replace the older RBC/UKQCD 12 results in our averages.

$N_f = 2 + 1$  MILC results for light-quark masses go back to 2004 [24, 75]. They use rooted staggered fermions. By 2009 their simulations covered an impressive range of parameter space, with lattice spacings which go down to 0.045 fm and valence-pion masses down to approximately 180 MeV [26]. The most recent MILC  $N_f = 2 + 1$  results, i.e. MILC 10A [69] and MILC 09A [26], feature large statistics and 2-loop renormalization. Since these data sets subsume those of their previous calculations, these latest results are the only ones that must be kept in any world average.

The PACS-CS 12 [67] calculation represents an important extension of the collaboration's earlier 2010 computation [5], which already probed pion masses down to  $M_\pi \simeq 135 \text{ MeV}$ , i.e. down to the physical-mass point. This was achieved by reweighting the simulations performed in PACS-CS 08 [3] at  $M_\pi \simeq 160 \text{ MeV}$ . If adequately controlled, this procedure eliminates the need to extrapolate to the physical-mass point and, hence, the corresponding systematic error.

Collaboration	Ref.	publication status	chiral extrapolation	continuum extrapolation	finite volume	renormalization	running	$m_{ud}$	$m_s$
RBC/UKQCD 14B <sup>⊖</sup>	[12]	P	★	★	★	★	<i>d</i>	3.31(4)(4)	90.3(0.9)(1.0)
RBC/UKQCD 12 <sup>⊖</sup>	[8]	A	★	○	★	★	<i>d</i>	3.37(9)(7)(1)(2)	92.3(1.9)(0.9)(0.4)(0.8)
PACS-CS 12 <sup>*</sup>	[67]	A	★	■	■	★	<i>b</i>	3.12(24)(8)	83.60(0.58)(2.23)
Laiho 11	[68]	C	○	★	★	○	–	3.31(7)(20)(17)	94.2(1.4)(3.2)(4.7)
BMW 10A, 10B <sup>+</sup>	[6, 7]	A	★	★	★	★	<i>c</i>	3.469(47)(48)	95.5(1.1)(1.5)
PACS-CS 10	[5]	A	★	■	■	★	<i>b</i>	2.78(27)	86.7(2.3)
MILC 10A	[69]	C	○	★	★	○	–	3.19(4)(5)(16)	–
HPQCD 10 <sup>*</sup>	[66]	A	○	★	★	–	–	3.39(6)	92.2(1.3)
RBC/UKQCD 10A	[70]	A	○	○	★	★	<i>a</i>	3.59(13)(14)(8)	96.2(1.6)(0.2)(2.1)
Blum 10 <sup>†</sup>	[20]	A	○	■	○	★	–	3.44(12)(22)	97.6(2.9)(5.5)
PACS-CS 09	[4]	A	★	■	■	★	<i>b</i>	2.97(28)(3)	92.75(58)(95)
HPQCD 09A <sup>⊕</sup>	[71]	A	○	★	★	–	–	3.40(7)	92.4(1.5)
MILC 09A	[26]	C	○	★	★	○	–	3.25 (1)(7)(16)(0)	89.0(0.2)(1.6)(4.5)(0.1)
MILC 09	[25]	A	○	★	★	○	–	3.2(0)(1)(2)(0)	88(0)(3)(4)(0)
PACS-CS 08	[3]	A	★	■	■	■	–	2.527(47)	72.72(78)
RBC/UKQCD 08	[72]	A	○	■	★	★	–	3.72(16)(33)(18)	107.3(4.4)(9.7)(4.9)
CP-PACS/ JLQCD 07	[73]	A	■	★	★	■	–	3.55(19) <sup>(+56)</sup> <sub>(-20)</sub>	90.1(4.3) <sup>(+16.7)</sup> <sub>(-4.3)</sub>
HPQCD 05	[74]	A	○	○	○	○	–	3.2(0)(2)(2)(0) <sup>‡</sup>	87(0)(4)(4)(0) <sup>‡</sup>
MILC 04, HPQCD/ MILC/UKQCD 04	[24, 75]	A	○	○	○	■	–	2.8(0)(1)(3)(0)	76(0)(3)(7)(0)

⊖ The results are given in the  $\overline{\text{MS}}$  scheme at 3 instead of 2 GeV. We run them down to 2 GeV using numerically integrated 4-loop running [76, 77] with  $N_f = 3$  and with the values of  $\alpha_s(M_Z)$ ,  $m_b$  and  $m_c$  taken from Ref. [78]. The running factor is 1.106. At three loops it is only 0.2% smaller, indicating that running uncertainties are small. We neglect them here.

\* The calculation includes e.m. and  $m_u \neq m_d$  effects through reweighting.

† The fermion action used is tree-level improved.

\* What is calculated is then obtained by combining this result with HPQCD 09A's  $m_c/m_s = 11.85(16)$  [71]. Finally,  $m_{ud}$  is determined from  $m_s$  with the MILC 09 result for  $m_s/m_{ud}$ . Since  $m_c/m_s$  is renormalization group invariant in QCD, the renormalization and running of the quark masses enter indirectly through that of  $m_c$  (see below).

† The calculation includes quenched e.m. effects.

⊕ What is calculated is  $m_c/m_s = 11.85(16)$ .  $m_s$  is then obtained by combing this result with the determination  $m_c(m_c) = 1.268(9)$  GeV from Ref. [79]. Finally,  $m_{ud}$  is determined from  $m_s$  with the MILC 09 result for  $m_s/m_{ud}$ .

‡ The bare numbers are those of MILC 04. The masses are simply rescaled, using the ratio of the 2-loop to 1-loop renormalization factors.

*a* The masses are renormalized nonperturbatively at a scale of 2 GeV in a couple of  $N_f = 3$  RI/SMOM schemes. A careful study of perturbative matching uncertainties has been performed by comparing results in the two schemes in the region of 2 GeV to 3 GeV [70].

*b* The masses are renormalized and run nonperturbatively up to a scale of 40 GeV in the  $N_f = 3$  SF scheme. In this scheme, nonperturbative and NLO running for the quark masses are shown to agree well from 40 GeV all the way down to 3 GeV [5].

*c* The masses are renormalized and run nonperturbatively up to a scale of 4 GeV in the  $N_f = 3$  RI/MOM scheme. In this scheme, nonperturbative and N<sup>3</sup>LO running for the quark masses are shown to agree from 6 GeV down to 3 GeV to better than 1% [7].

*d* All required running is performed nonperturbatively.

Table 4:  $N_f = 2 + 1$  lattice results for the masses  $m_{ud}$  and  $m_s$  (see Tab. 3 for notation).

The new calculation now applies similar reweighting techniques to include electromagnetic and  $m_u \neq m_d$  isospin-breaking effects directly at the physical pion mass. Further, as in PACS-CS 10 [5], renormalization of quark masses is implemented nonperturbatively, through the Schrödinger functional method [80]. As it stands, the main drawback of the calculation, which makes the inclusion of its results in a world average of lattice results inappropriate at this stage, is that for the lightest quark mass the volume is very small, corresponding to  $LM_\pi \simeq 2.0$ , a value for which finite-volume effects will be difficult to control. Another problem is that the calculation was performed at a single lattice spacing, forbidding a continuum extrapolation. Further, it is unclear at this point what might be the systematic errors associated with the reweighting procedure.

The BMW 10A, 10B [6, 7] calculation still satisfies our stricter selection criteria. They reach the physical up- and down-quark mass by *interpolation* instead of by extrapolation. Moreover, their calculation was performed at five lattice spacings ranging from 0.054 to 0.116 fm, with full nonperturbative renormalization and running and in volumes of up to  $(6 \text{ fm})^3$  guaranteeing that the continuum limit, renormalization and infinite-volume extrapolation are controlled. It does neglect, however, isospin-breaking effects, which are small on the scale of their error bars.

Finally we come to another calculation which satisfies our selection criteria, HPQCD 10 [66]. It updates the staggered fermions calculation of HPQCD 09A [71]. In these papers the renormalized mass of the strange quark is obtained by combining the result of a precise calculation of the renormalized charm-quark mass,  $m_c$ , with the result of a calculation of the quark-mass ratio,  $m_c/m_s$ . As described in Ref. [79] and in Sec. 3.2, HPQCD determines  $m_c$  by fitting Euclidean-time moments of the  $\bar{c}c$  pseudoscalar density two-point functions, obtained numerically in lattice QCD, to fourth-order, continuum perturbative expressions. These moments are normalized and chosen so as to require no renormalization with staggered fermions. Since  $m_c/m_s$  requires no renormalization either, HPQCD's approach displaces the problem of lattice renormalization in the computation of  $m_s$  to one of computing continuum perturbative expressions for the moments. To calculate  $m_{ud}$  HPQCD 10 [66] use the MILC 09 determination of the quark-mass ratio  $m_s/m_{ud}$  [25].

HPQCD 09A [71] obtains  $m_c/m_s = 11.85(16)$  [71] fully nonperturbatively, with a precision slightly larger than 1%. HPQCD 10's determination of the charm-quark mass,  $m_c(m_c) = 1.268(6)$ ,<sup>3</sup> is even more precise, achieving an accuracy better than 0.5%. While these errors are, perhaps, surprisingly small, we take them at face value as we do those of RBC/UKQCD 14, since we will add a 2% error due to the quenching of the charm on the final result.

This discussion leaves us with four results for our final average for  $m_s$ : MILC 09A [26], BMW 10A, 10B [6, 7], HPQCD 10 [66] and RBC/UKQCD 14 [12]. Assuming that the result from HPQCD 10 is 100% correlated with that of MILC 09A, as it is based on a subset of the MILC 09A configurations, we find  $m_s = 92.0(1.1)$  MeV with a  $\chi^2/\text{dof} = 1.8$ .

For the light quark mass  $m_{ud}$ , the results satisfying our criteria are RBC/UKQCD 14B, BMW 10A, 10B, HPQCD 10, and MILC 10A. For the error, we include the same 100% correlation between statistical errors for the latter two as for the strange case, resulting in  $m_{ud} = 3.373(43)$  at 2 GeV in the  $\overline{\text{MS}}$  scheme ( $\chi^2/\text{d.of.}=1.5$ ). Adding the 2% estimate for the

<sup>3</sup>To obtain this number, we have used the conversion from  $\mu = 3 \text{ GeV}$  to  $m_c$  given in Ref. [79].

missing charm contribution, our final estimates for the light-quark masses are

$$N_f = 2 + 1 : \quad \begin{aligned} m_{ud} &= 3.373(80) \text{ MeV} && \text{Refs. [6, 7, 12, 66, 69]}, \\ m_s &= 92.0(2.1) \text{ MeV} && \text{Refs. [6, 7, 12, 26, 66]}. \end{aligned} \quad (18)$$

$N_f = 2 + 1 + 1$  lattice calculations

One of the novelties since the last edition of this review [2] is the fact that  $N_f = 2 + 1 + 1$  results for the light-quark masses have been published. These and the features of the corresponding calculations are summarized in Tab. 5. Note that the results of Ref. [11] are reported as  $m_s(2 \text{ GeV}; N_f = 3)$  and those of Ref. [9] as  $m_{ud(s)}(2 \text{ GeV}; N_f = 4)$ . We convert the former to  $N_f = 4$  and obtain  $m_s(2 \text{ GeV}; N_f = 4) = 93.7(8) \text{ MeV}$ . The average of ETM 14 and HPQCD 14A is  $93.9(1.1) \text{ MeV}$  with  $\chi^2/\text{d.o.f.} = 1.8$ . For the light0quark average we use the sole available value from ETM 14A. Our averages are

$$N_f = 2 + 1 + 1 : \quad \begin{aligned} m_{ud} &= 3.70(17) \text{ MeV} && \text{Ref. [9]}, \\ m_s &= 93.9(1.1) \text{ MeV} && \text{Refs. [9, 11]}. \end{aligned} \quad (19)$$

Collaboration	Ref.	publication status	chiral extrapolation	continuum extrapolation	finite volume	renormalization	running	$m_{ud}$	$m_s$
HPQCD 14A <sup>⊕</sup>	[11]	A	★	★	★	–	–		93.7(8)
ETM 14 <sup>⊕</sup>	[9]	A	○	★	★	★	–	3.70(13)(11)	99.6(3.6)(2.3)

<sup>⊕</sup> As explained in the text,  $m_s$  is obtained by combining the results  $m_c(5 \text{ GeV}; N_f = 4) = 0.8905(56) \text{ GeV}$  and  $(m_c/m_s)(N_f = 4) = 11.652(65)$ , determined on the same data set. A subsequent scale and scheme conversion, performed by the authors leads, to the value  $93.6(8)$ . In the table we have converted this to  $m_s(2 \text{ GeV}; N_f = 4)$ , which makes a very small change.

Table 5:  $N_f = 2 + 1 + 1$  lattice results for the masses  $m_{ud}$  and  $m_s$  (see Tab. 3 for notation).

In Figs. 1 and 2 the lattice results listed in Tabs. 3, 4 and 5 and the FLAG averages obtained at each value of  $N_f$  are presented and compared with various phenomenological results.

### 3.1.4 Lattice determinations of $m_s/m_{ud}$

The lattice results for  $m_s/m_{ud}$  are summarized in Tab. 6. In the ratio  $m_s/m_{ud}$ , one of the sources of systematic error – the uncertainties in the renormalization factors – drops out. Also, we can compare the lattice results with the leading-order formula of  $\chi\text{PT}$ ,

$$\frac{m_s}{m_{ud}} \stackrel{\text{LO}}{=} \frac{\hat{M}_{K^+}^2 + \hat{M}_{K^0}^2 - \hat{M}_{\pi^+}^2}{\hat{M}_{\pi^+}^2}, \quad (20)$$

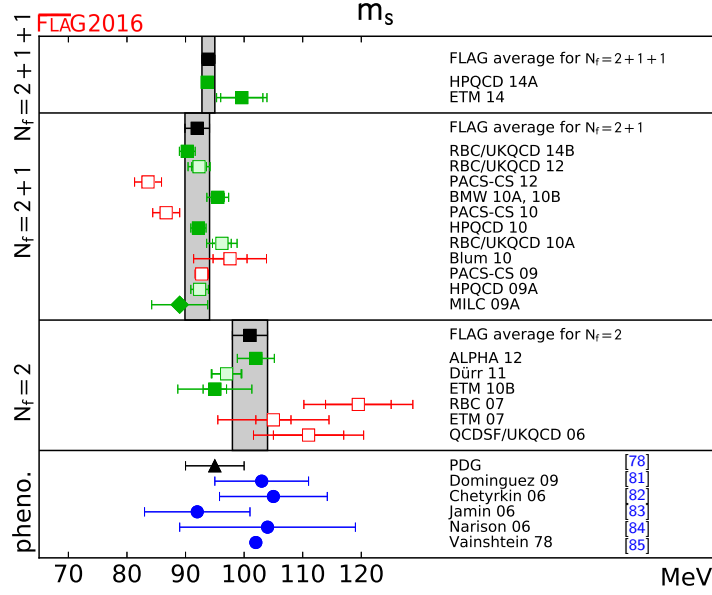


Figure 1:  $\overline{\text{MS}}$  mass of the strange quark (at 2 GeV scale) in MeV. The upper three panels show the lattice results listed in Tabs. 3, 4 and 5, while the bottom panel collects a few sum rule results and also indicates the current PDG estimate. Diamonds and squares represent results based on perturbative and nonperturbative renormalization, respectively. The black squares and the grey bands represent our estimates (17), (18) and (19). The significance of the colours is explained in Sec. 2.

which relates the quantity  $m_s/m_{ud}$  to a ratio of meson masses in QCD. Expressing these in terms of the physical masses and the four coefficients introduced in Eqs. (10)-(12), linearizing the result with respect to the corrections and inserting the observed mass values, we obtain

$$\frac{m_s}{m_{ud}} \stackrel{\text{LO}}{=} 25.9 - 0.1 \epsilon + 1.9 \epsilon_{\pi^0} - 0.1 \epsilon_{K^0} - 1.8 \epsilon_m. \quad (21)$$

If the coefficients  $\epsilon$ ,  $\epsilon_{\pi^0}$ ,  $\epsilon_{K^0}$  and  $\epsilon_m$  are set equal to zero, the right hand side reduces to the value  $m_s/m_{ud} = 25.9$  that follows from Weinberg's leading-order formulae for  $m_u/m_d$  and  $m_s/m_d$  [88], in accordance with the fact that these do account for the e.m. interaction at leading chiral order, and neglect the mass difference between the charged and neutral pions in QCD. Inserting the estimates (13) gives the effect of chiral corrections to the e.m. self-energies and of the mass difference between the charged and neutral pions in QCD. With these, the LO prediction in QCD becomes

$$\frac{m_s}{m_{ud}} \stackrel{\text{LO}}{=} 25.9(1), \quad (22)$$

leaving the central value unchanged at 25.9. The corrections parameterized by the coefficients of Eq. (13) are small for this quantity. Note that the quoted uncertainty does not include an estimate of higher-order chiral contributions to this LO QCD formula, but only accounts for the error bars in the coefficients. However, even this small uncertainty is no longer irrelevant given the the high precision reached in lattice determinations of the ratio  $m_s/m_{ud}$ .

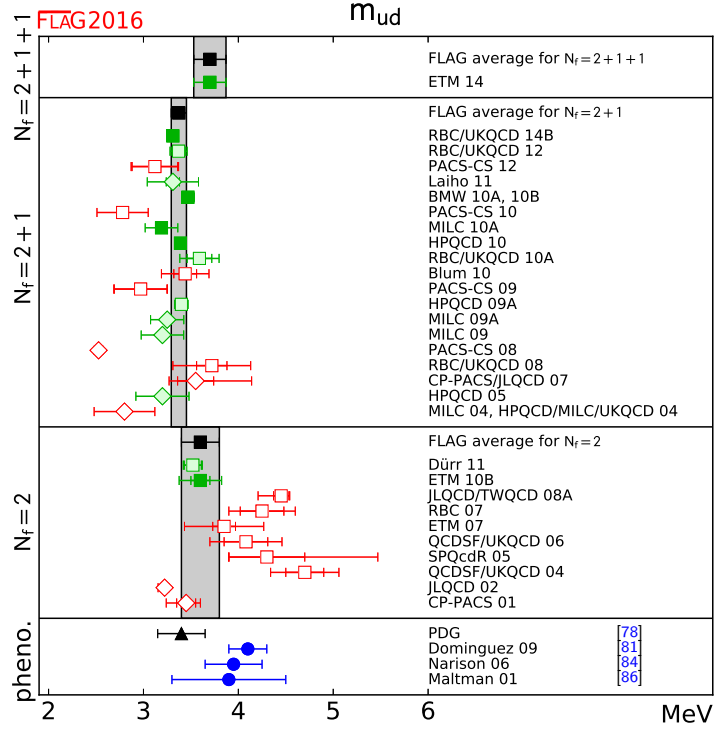


Figure 2: Mean mass of the two lightest quarks,  $m_{ud} = \frac{1}{2}(m_u + m_d)$  (for details see Fig. 1).

The lattice results in Tab. 6, which satisfy our selection criteria, indicate that the corrections generated by the nonleading terms of the chiral perturbation series are remarkably small, in the range 3–10%. Despite the fact that the  $SU(3)$ -flavour-symmetry breaking effects in the Nambu-Goldstone boson masses are very large ( $M_K^2 \simeq 13 M_\pi^2$ ), the mass spectrum of the pseudoscalar octet obeys the  $SU(3) \times SU(3)$  formula (20) very well.

#### $N_f = 2$ lattice calculations

With respect to the FLAG 13 review [2] there is only one new result, ETM 14D [87], based on recent ETM gauge ensembles generated close to the physical point with the addition of a clover term to the tmQCD action. The new simulations are performed at a single lattice spacing of  $\simeq 0.09$  fm and at a single box size  $L \simeq 4$  fm and therefore their calculations do not pass our criteria for the continuum extrapolation and finite-volume effects.

Therefore the FLAG average at  $N_f = 2$  is still obtained by considering only the ETM 10B result (described already in the previous Section), namely

$$N_f = 2 : \quad m_s/m_{ud} = 27.3 \quad (9) \quad \text{Ref. [54],} \quad (23)$$

with an overall uncertainty equal to 3.3%.

Collaboration	Ref.	$N_f$	publication status	chiral extrapolation	continuum extrapolation	finite volume	$m_s/m_{ud}$
FNAL/MILC 14A	[10]	2+1+1	A	★	★	★	27.35(5) $^{+10}_{-7}$
ETM 14	[9]	2+1+1	A	○	★	○	26.66(32)(2)
RBC/UKQCD 14B	[12]	2+1	P	★	★	★	27.34(21)
RBC/UKQCD 12 <sup>⊖</sup>	[8]	2+1	A	★	○	★	27.36(39)(31)(22)
PACS-CS 12*	[67]	2+1	A	★	■	■	26.8(2.0)
Laiho 11	[68]	2+1	C	○	★	★	28.4(0.5)(1.3)
BMW 10A, 10B <sup>+</sup>	[6, 7]	2+1	A	★	★	★	27.53(20)(8)
RBC/UKQCD 10A	[70]	2+1	A	○	○	★	26.8(0.8)(1.1)
Blum 10 <sup>†</sup>	[20]	2+1	A	○	■	○	28.31(0.29)(1.77)
PACS-CS 09	[4]	2+1	A	★	■	■	31.2(2.7)
MILC 09A	[26]	2+1	C	○	★	★	27.41(5)(22)(0)(4)
MILC 09	[25]	2+1	A	○	★	★	27.2(1)(3)(0)(0)
PACS-CS 08	[3]	2+1	A	★	■	■	28.8(4)
RBC/UKQCD 08	[72]	2+1	A	○	■	★	28.8(0.4)(1.6)
MILC 04, HPQCD/ MILC/UKQCD 04	[24, 75]	2+1	A	○	○	○	27.4(1)(4)(0)(1)
ETM 14D	[87]	2	C	★	■	■	27.63(13)
ETM 10B	[54]	2	A	○	★	○	27.3(5)(7)
RBC 07 <sup>†</sup>	[22]	2	A	■	■	★	28.10(38)
ETM 07	[56]	2	A	○	■	○	27.3(0.3)(1.2)
QCDSF/UKQCD 06	[62]	2	A	■	★	■	27.2(3.2)

⊖ The errors are statistical, chiral and finite volume.

\* The calculation includes e.m. and  $m_u \neq m_d$  effects through reweighting.

+ The fermion action used is tree-level improved.

† The calculation includes quenched e.m. effects.

Table 6: Lattice results for the ratio  $m_s/m_{ud}$ .

### $N_f = 2 + 1$ lattice calculations

For  $N_f = 2 + 1$  our average of  $m_s/m_{ud}$  is based on the new result RBC/UKQCD 14B, which replaces RBC/UKQCD 12 (see Sec. 3.1.3), and on the results MILC 09A and BMW 10A, 10B. The value quoted by HPQCD 10 does not represent independent information as it relies on the result for  $m_s/m_{ud}$  obtained by the MILC collaboration. Averaging these results according to the prescriptions of Sec. 2.3 gives  $m_s/m_{ud} = 27.43(13)$  with  $\chi^2/\text{dof} \simeq 0.2$ . Since the errors associated with renormalization drop out in the ratio, the uncertainties are even smaller than in the case of the quark masses themselves: the above number for  $m_s/m_{ud}$  amounts to an accuracy of 0.5%.

At this level of precision, the uncertainties in the electromagnetic and strong isospin-breaking corrections are not completely negligible. The error estimate in the LO result (22)



indicates the expected order of magnitude. In view of this, we ascribe conservatively a 1.0% uncertainty to this source of error. Thus, our final conservative estimate is

$$N_f = 2 + 1 : \quad m_s/m_{ud} = 27.43 \text{ (13) (27) } = 27.43 \text{ (31)} \quad \text{Ref. [6, 7, 12, 26]}, \quad (24)$$

with a total 1.1% uncertainty. It is also fully consistent with the ratio computed from our individual quark masses in Eq. (18),  $m_s/m_{ud} = 27.6(6)$ , which has a larger 2.2% uncertainty. In Eq. (24) the first error comes from the averaging of the lattice results, and the second is the one that we add to account for the neglect of isospin-breaking effects.

#### $N_f = 2 + 1 + 1$ lattice calculations

For  $N_f = 2 + 1 + 1$  there are two results, ETM 14 [9] and FNAL/MILC 14A [10], both of which satisfy our selection criteria.

ETM 14 uses 15 twisted mass gauge ensembles at 3 lattice spacings ranging from 0.062 to 0.089 fm (using  $f_\pi$  as input), in boxes of size ranging from 2.0 to 3.0 fm and pion masses from 210 to 440 MeV (explaining the tag  $\circ$  in the chiral extrapolation and the tag  $\star$  for the continuum extrapolation). The value of  $M_\pi L$  at their smallest pion mass is 3.2 with more than two volumes (explaining the tag  $\circ$  in the finite-volume effects). They fix the strange mass with the kaon mass.

FNAL/MILC 14A employs HISQ staggered fermions. Their result is based on 21 ensembles at 4 values of the coupling  $\beta$  corresponding to lattice spacings in the range from 0.057 to 0.153 fm, in boxes of sizes up to 5.8 fm and with taste-Goldstone pion masses down to 130 MeV and RMS pion masses down to 143 MeV. They fix the strange mass with  $M_{\bar{s}s}$ , corrected for e.m. effects with  $\bar{\epsilon} = 0.84(20)$  [32]. All of our selection criteria are satisfied with the tag  $\star$ . Thus our average is given by  $m_s/m_{ud} = 27.30(20)$ , where the error includes a large stretching factor equal to  $\sqrt{\chi^2/\text{dof}} \simeq 2.1$ , coming from our rules for the averages discussed in Sec. 2.2. Nevertheless the above number amounts still to an accuracy of 0.7%. As in the case of our average for  $N_f = 2 + 1$ , we add a 1.0% uncertainty related to the neglect of isospin-breaking effects, leading to

$$N_f = 2 + 1 + 1 : \quad m_s/m_{ud} = 27.30 \text{ (20) (27) } = 27.30 \text{ (34)} \quad \text{Refs. [9, 10]}, \quad (25)$$

which corresponds to an overall uncertainty equal to 1.3%.

All the lattice results listed in Tab. 6 as well as the FLAG averages for each value of  $N_f$  are reported in Fig. 3 and compared with  $\chi$ PT, sum rules and the updated PDG estimate  $m_s/m_{ud} = 27.5(3)$  [78].

Note that our averages (23), (24) and (25), obtained for  $N_f = 2, 2 + 1$  and  $2 + 1 + 1$ , respectively, agree very well within the quoted errors. They also show that the LO prediction of  $\chi$ PT in Eq. (22) receives only small corrections from higher orders of the chiral expansion: according to Eqs. (24) and (25), these generate shifts of 5.9(1.1)% and 5.4(1.2)% relative to Eq. (22), respectively.

The ratio  $m_s/m_{ud}$  can also be extracted from the masses of the neutral Nambu-Goldstone bosons: neglecting effects of order  $(m_u - m_d)^2$  also here, the leading-order formula reads  $m_s/m_{ud} \stackrel{\text{LO}}{=} \frac{3}{2} \hat{M}_\eta^2 / \hat{M}_\pi^2 - \frac{1}{2}$ . Numerically, this gives  $m_s/m_{ud} \stackrel{\text{LO}}{=} 24.2$ . The relation has the advantage that the e.m. corrections are expected to be much smaller here, but it is more difficult to calculate the  $\eta$ -mass on the lattice. The comparison with Eqs. (24) and (25) shows that, in this case, the NLO contributions are somewhat larger: 11.9(9)% and 11.4(1.1)%.

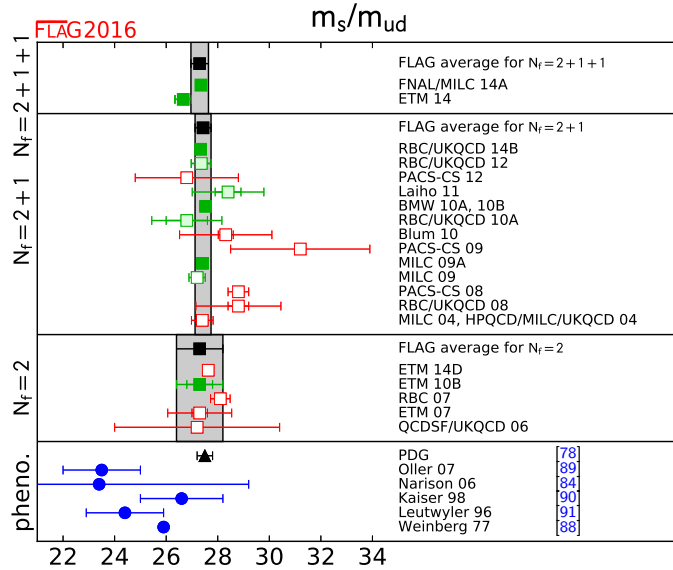


Figure 3: Results for the ratio  $m_s/m_{ud}$ . The upper part indicates the lattice results listed in Tab. 6 together with the FLAG averages for each value of  $N_f$ . The lower part shows results obtained from  $\chi$ PT and sum rules, together with the current PDG estimate.

### 3.1.5 Lattice determination of $m_u$ and $m_d$

Since FLAG 13, two new results have been reported for nondegenerate light-quark masses, ETM 14 [9], and QCDSF/UKQCD 15 [92], for  $N_f = 2 + 1 + 1$ , and 3 flavours respectively. The former uses simulations in pure QCD, but determines  $m_u - m_d$  from the slope of the square of the kaon mass and the neutral-charged mass-squares difference, evaluated at the isospin-symmetric point. The latter uses QCD+QED dynamical simulations performed at the  $SU(3)$ -flavour-symmetric point, but at a single lattice spacing, so they do not enter our average. While QCDSF/UKQCD 15 use three volumes, the smallest has linear size roughly 1.7 fm, and the smallest partially quenched pion mass is greater than 200 MeV, so our finite-volume and chiral-extrapolation criteria require  $\circ$  ratings. In Ref. [92] results for  $\epsilon$  and  $m_u/m_d$  are computed in the so-called Dashen scheme. A subsequent paper [38] gives formulae to convert the  $\epsilon$  parameters to the  $\overline{\text{MS}}$  scheme.

As the above implies, the determination of  $m_u$  and  $m_d$  separately requires additional input. MILC 09A [26] uses the mass difference between  $K^0$  and  $K^+$ , from which they subtract electromagnetic effects using Dashen’s theorem with corrections, as discussed in Sec. 3.1.1. The up and down sea quarks remain degenerate in their calculation, fixed to the value of  $m_{ud}$  obtained from  $M_{\pi^0}$ .

To determine  $m_u/m_d$ , BMW 10A, 10B [6, 7] follow a slightly different strategy. They obtain this ratio from their result for  $m_s/m_{ud}$  combined with a phenomenological determination of the isospin-breaking quark-mass ratio  $Q = 22.3(8)$ , defined below in Eq. (32), from  $\eta \rightarrow 3\pi$  decays [18] (the decay  $\eta \rightarrow 3\pi$  is very sensitive to QCD isospin breaking but fairly insensitive to QED isospin breaking). As discussed in Sec. 3.1.6, the central value of the e.m. parameter

$\epsilon$  in Eq. (13) is taken from the same source.

RM123 11 [93] actually uses the e.m. parameter  $\epsilon = 0.7(5)$  from the first edition of the FLAG review [44]. However they estimate the effects of strong isospin breaking at first non-trivial order, by inserting the operator  $\frac{1}{2}(m_u - m_d) \int (\bar{u}u - \bar{d}d)$  into correlation functions, while performing the gauge averages in the isospin limit. Applying these techniques, they obtain  $(\hat{M}_{K^0}^2 - \hat{M}_{K^+}^2)/(m_d - m_u) = 2.57(8)$  MeV. Combining this result with the phenomenological  $(\hat{M}_{K^0}^2 - \hat{M}_{K^+}^2) = 6.05(63) \times 10^3$  determined with the above value of  $\epsilon$ , they get  $(m_d - m_u) = 2.35(8)(24)$  MeV, where the first error corresponds to the lattice statistical and systematic uncertainties combined in quadrature, while the second arises from the uncertainty on  $\epsilon$ . Note that below we quote results from RM123 11 for  $m_u$ ,  $m_d$  and  $m_u/m_d$ . As described in Tab. 7, we obtain them by combining RM123 11's result for  $(m_d - m_u)$  with ETM 10B's result for  $m_{ud}$ .

Instead of subtracting electromagnetic effects using phenomenology, RBC 07 [22] and Blum 10 [20] actually include a quenched electromagnetic field in their calculation. This means that their results include corrections to Dashen's theorem, albeit only in the presence of quenched electromagnetism. Since the up and down quarks in the sea are treated as degenerate, very small isospin corrections are neglected, as in MILC's calculation.

PACS-CS 12 [67] takes the inclusion of isospin-breaking effects one step further. Using reweighting techniques, it also includes electromagnetic and  $m_u - m_d$  effects in the sea.

Lattice results for  $m_u$ ,  $m_d$  and  $m_u/m_d$  are summarized in Tab. 7. In order to discuss them, we consider the LO formula

$$\frac{m_u}{m_d} \stackrel{\text{LO}}{=} \frac{\hat{M}_{K^+}^2 - \hat{M}_{K^0}^2 + \hat{M}_{\pi^+}^2}{\hat{M}_{K^0}^2 - \hat{M}_{K^+}^2 + \hat{M}_{\pi^+}^2}. \quad (26)$$

Using Eqs. (10)–(12) to express the meson masses in QCD in terms of the physical ones and linearizing in the corrections, this relation takes the form

$$\frac{m_u}{m_d} \stackrel{\text{LO}}{=} 0.558 - 0.084\epsilon - 0.02\epsilon_{\pi^0} + 0.11\epsilon_m. \quad (27)$$

Inserting the estimates (13) and adding errors in quadrature, the LO prediction becomes

$$\frac{m_u}{m_d} \stackrel{\text{LO}}{=} 0.50(3). \quad (28)$$

Again, the quoted error exclusively accounts for the errors attached to the estimates (13) for the epsilons – contributions of nonleading order are ignored. The uncertainty in the leading-order prediction is dominated by the one in the coefficient  $\epsilon$ , which specifies the difference between the meson squared-mass splittings generated by the e.m. interaction in the kaon and pion multiplets. The reduction in the error on this coefficient since the previous review [44] results in a reduction of a factor of a little less than 2 in the uncertainty on the LO value of  $m_u/m_d$  given in Eq. (28).

It is interesting to compare the assumptions made or results obtained by the different collaborations for the violation of Dashen's theorem. The input used in MILC 09A is  $\epsilon = 1.2(5)$  [26], while the  $N_f = 2$  computation of RM123 13 finds  $\epsilon = 0.79(18)(18)$  [37]. As discussed in Sec. 3.1.6, the value of  $Q$  used by BMW 10A, 10B [6, 7] gives  $\epsilon = 0.70(28)$  at NLO (see Eq. (40)). On the other hand, RBC 07 [22] and Blum 10 [20] obtain the results  $\epsilon = 0.13(4)$  and  $\epsilon = 0.5(1)$ . The new results from QCDSF/UKQCD 15 give  $\epsilon = 0.50(6)$  [38].

Collaboration	Ref.	publication status chiral extrapolation continuum extrapolation finite volume renormalization running	$m_u$	$m_d$	$m_u/m_d$
MILC 14	[32]	C ★ ★ ★ – –			0.4482(48)( $^{+21}_{-115}$ )(1)(165)
ETM 14	[9]	A ★ ★ ★ ★ b	2.36(24)	5.03(26)	0.470(56)
QCDSF/UKQCD 15 <sup>⊖</sup>	[92]	P ○ ■ ○ – –			0.52(5)
PACS-CS 12 <sup>*</sup>	[67]	A ★ ■ ■ ★ a	2.57(26)(7)	3.68(29)(10)	0.698(51)
Laiho 11	[68]	C ○ ★ ★ ○ –	1.90(8)(21)(10)	4.73(9)(27)(24)	0.401(13)(45)
HPQCD 10 <sup>‡</sup>	[66]	A ○ ★ ★ ★ –	2.01(14)	4.77(15)	
BMW 10A, 10B <sup>+</sup>	[6, 7]	A ★ ★ ★ ★ b	2.15(03)(10)	4.79(07)(12)	0.448(06)(29)
Blum 10 <sup>†</sup>	[20]	A ○ ■ ○ ○ –	2.24(10)(34)	4.65(15)(32)	0.4818(96)(860)
MILC 09A	[26]	C ○ ★ ★ ○ –	1.96(0)(6)(10)(12)	4.53(1)(8)(23)(12)	0.432(1)(9)(0)(39)
MILC 09	[25]	A ○ ★ ★ ○ –	1.9(0)(1)(1)(1)	4.6(0)(2)(2)(1)	0.42(0)(1)(0)(4)
MILC 04, HPQCD/ MILC/UKQCD 04	[24] [75]	A ○ ○ ○ ■ –	1.7(0)(1)(2)(2)	3.9(0)(1)(4)(2)	0.43(0)(1)(0)(8)
RM123 13	[37]	A ○ ★ ○ ★ c	2.40(15)(17)	4.80 (15)(17)	0.50(2)(3)
RM123 11 <sup>⊕</sup>	[93]	A ○ ★ ○ ★ c	<i>2.43(11)(23)</i>	<i>4.78(11)(23)</i>	<i>0.51(2)(4)</i>
Dürr 11 <sup>*</sup>	[55]	A ○ ★ ○ – –	2.18(6)(11)	4.87(14)(16)	
RBC 07 <sup>†</sup>	[22]	A ■ ■ ★ ★ –	3.02(27)(19)	5.49(20)(34)	0.550(31)

⊖ Results are computed in QCD+QED and quoted in an unconventional “Dashen scheme”.

\* The calculation includes e.m. and  $m_u \neq m_d$  effects through reweighting.

‡ Values obtained by combining the HPQCD 10 result for  $m_s$  with the MILC 09 results for  $m_s/m_{ud}$  and  $m_u/m_d$ .

+ The fermion action used is tree-level improved.

\* Values obtained by combining the Dürr 11 result for  $m_s$  with the BMW 10A, 10B results for  $m_s/m_{ud}$  and  $m_u/m_d$ .

⊕ The results presented on this line are in italics because they do not appear in the quoted paper. Rather, the values for  $m_u$ ,  $m_d$  and  $m_u/m_d$  are obtained by combining the result of RM123 11 for  $(m_d - m_u)$  [93] with  $m_{ud} = 3.6(2)$  MeV from ETM 10B.  $(m_d - m_u) = 2.35(8)(24)$  MeV in Ref. [93] was obtained assuming  $\epsilon = 0.7(5)$  [44] and  $\epsilon_m = \epsilon_{\pi^0} = \epsilon_{K^0} = 0$ . In the quoted results, the first error corresponds to the lattice statistical and systematic errors combined in quadrature, while the second arises from the uncertainties associated with  $\epsilon$ .

† The calculation includes quenched e.m. effects.

a The masses are renormalized and run nonperturbatively up to a scale of 100 GeV in the  $N_f = 2$  SF scheme. In this scheme, nonperturbative and NLO running for the quark masses are shown to agree well from 100 GeV all the way down to 2 GeV [58].

b The masses are renormalized and run nonperturbatively up to a scale of 4 GeV in the  $N_f = 3$  RI/MOM scheme. In this scheme, nonperturbative and N<sup>3</sup>LO running for the quark masses are shown to agree from 6 GeV down to 3 GeV to better than 1% [7].

c The masses are renormalized nonperturbatively at scales  $1/a \sim 2 \div 3$  GeV in the  $N_f = 2$  RI/MOM scheme. In this scheme, nonperturbative and N<sup>3</sup>LO running for the quark masses are shown to agree from 4 GeV down 2 GeV to better than 3% [65].

Table 7: Lattice results for  $m_u$ ,  $m_d$  (MeV) and for the ratio  $m_u/m_d$ . The values refer to the  $\overline{\text{MS}}$  scheme at scale 2 GeV. The top part of the table lists the result obtained with  $N_f = 2 + 1 + 1$ , while the middle and lower part presents calculations with  $N_f = 2 + 1$  and  $N_f = 2$ , respectively.

Note that PACS-CS 12 [67] do not provide results which allow us to determine  $\epsilon$  directly. However, using their result for  $m_u/m_d$ , together with Eq. (27), and neglecting NLO terms, one finds  $\epsilon = -1.6(6)$ , which is difficult to reconcile with what is known from phenomenology (see Secs. 3.1.1 and 3.1.6). Since the values assumed or obtained for  $\epsilon$  differ, it does not come as a surprise that the determinations of  $m_u/m_d$  are different.

These values of  $\epsilon$  are also interesting because they allow us to estimate the chiral corrections to the LO prediction (28) for  $m_u/m_d$ . Indeed, evaluating the relation (27) for the values of  $\epsilon$  given above, and neglecting all other corrections in this equation, yields the LO values  $(m_u/m_d)^{\text{LO}} = 0.46(4)$ ,  $0.547(3)$ ,  $0.52(1)$ ,  $0.50(2)$ ,  $0.49(2)$  and  $0.51(1)$  for MILC 09A, RBC 07, Blum 10, BMW 10A, 10B, RM123 13, and QCDSF/UKQCD 15, respectively. However, in comparing these numbers to the nonperturbative results of Tab. 7 one must be careful not to double count the uncertainty arising from  $\epsilon$ . One way to obtain a sharp comparison is to consider the ratio of the results of Tab. 7 to the LO values  $(m_u/m_d)^{\text{LO}}$ , in which the uncertainty from  $\epsilon$  cancels to good accuracy. Here we will assume for simplicity that they cancel completely and will drop all uncertainties related to  $\epsilon$ . For  $N_f = 2$  we consider RM123 13 [37], which updates RM123 11 and has no red dots. Since the uncertainties common to  $\epsilon$  and  $m_u/m_d$  are not explicitly given in Ref. [37], we have to estimate them. For that we use the leading-order result for  $m_u/m_d$ , computed with RM123 13's value for  $\epsilon$ . Its error bar is the contribution of the uncertainty on  $\epsilon$  to  $(m_u/m_d)^{\text{LO}}$ . To good approximation this contribution will be the same for the value of  $m_u/m_d$  computed in Ref. [37]. Thus, we subtract it in quadrature from RM123 13's result in Tab. 7 and compute  $(m_u/m_d)/(m_u/m_d)^{\text{LO}}$ , dropping uncertainties related to  $\epsilon$ . We find  $(m_u/m_d)/(m_u/m_d)^{\text{LO}} = 1.02(6)$ . This result suggests that chiral corrections in the case of  $N_f = 2$  are negligible. For the two most accurate  $N_f = 2 + 1$  calculations, those of MILC 09A and BMW 10A, 10B, this ratio of ratios is  $0.94(2)$  and  $0.90(1)$ , respectively. Though these two numbers are not fully consistent within our rough estimate of the errors, they indicate that higher-order corrections to Eq. (28) are negative and about 8% when  $N_f = 2 + 1$ . In the following, we will take them to be  $-8(4)\%$ . The fact that these corrections are seemingly larger and of opposite sign than in the  $N_f = 2$  case is not understood at this point. It could be an effect associated with the quenching of the strange quark. It could also be due to the fact that the RM123 13 calculation does not probe deeply enough into the chiral regime – it has  $M_\pi \gtrsim 270$  MeV – to pick up on important chiral corrections. Of course, being less than a two-standard-deviation effect, it may be that there is no problem at all and that differences from the LO result are actually small.

Given the exploratory nature of the RBC 07 calculation, its results do not allow us to draw solid conclusions about the e.m. contributions to  $m_u/m_d$  for  $N_f = 2$ . As discussed in Sec. 3.1.3 and here, the  $N_f = 2 + 1$  results of Blum 10, PACS-CS 12, and QCDSF/UKQCD 15 do not pass our selection criteria either. We therefore resort to the phenomenological estimates of the electromagnetic self-energies discussed in Sec. 3.1.1, which are validated by recent, preliminary lattice results.

Since RM123 13 [37] includes a lattice estimate of e.m. corrections, for the  $N_f = 2$  final results we simply quote the values of  $m_u$ ,  $m_d$ , and  $m_u/m_d$  from RM123 13 given in Tab. 7:

$$\begin{array}{lll}
 N_f = 2 : & m_u = 2.40(23) \text{ MeV} & \text{Ref. [37],} \\
 & m_d = 4.80(23) \text{ MeV} & \text{Ref. [37],} \\
 & m_u/m_d = 0.50(4) & \text{Ref. [37],}
 \end{array} \tag{29}$$

with errors of roughly 10%, 5% and 8%, respectively. In these results, the errors are obtained

by combining the lattice statistical and systematic errors in quadrature.

For  $N_f = 2 + 1$  there is to date no final, published computation of e.m. corrections. Thus, we take the LO estimate for  $m_u/m_d$  of Eq. (28) and use the -8(4)% obtained above as an estimate of the size of the corrections from higher orders in the chiral expansion. This gives  $m_u/m_d = 0.46(3)$ . The two individual masses can then be worked out from the estimate (18) for their mean. Therefore, for  $N_f = 2 + 1$  we obtain:

$$\begin{aligned}
 N_f = 2 + 1 : \quad & m_u = 2.16(9)(7) \text{ MeV} , \\
 & m_d = 4.68(14)(7) \text{ MeV} , \\
 & m_u/m_d = 0.46(2)(2) .
 \end{aligned} \tag{30}$$

In these results, the first error represents the lattice statistical and systematic errors, combined in quadrature, while the second arises from the uncertainties associated with e.m. corrections of Eq. (13). The estimates in Eq. (30) have uncertainties of order 5%, 3% and 7%, respectively.

Finally, for four flavours we simply adopt the results of ETM 14A which meet all of our criteria.

$$\begin{aligned}
 N_f = 2 + 1 + 1 : \quad & m_u = 2.36(24) \text{ MeV} && \text{Ref. [9]} , \\
 & m_d = 5.03(26) \text{ MeV} && \text{Ref. [9]} , \\
 & m_u/m_d = 0.470(56) && \text{Ref. [9]} .
 \end{aligned} \tag{31}$$

Naively propagating errors to the end, we obtain  $(m_u/m_d)_{N_f=2}/(m_u/m_d)_{N_f=2+1} = 1.09(10)$ . If instead of Eq. (29) we use the results from RM123 11, modified by the e.m. corrections in Eq. (13), as was done in our previous review, we obtain  $(m_u/m_d)_{N_f=2}/(m_u/m_d)_{N_f=2+1} = 1.11(7)(1)$ , confirming again the strong cancellation of e.m. uncertainties in the ratio. The  $N_f = 2$  and  $2 + 1$  results are compatible at the 1 to 1.5  $\sigma$  level. Clearly the difference between three and four flavours is even smaller, and completely covered by the quoted uncertainties.

It is interesting to note that in the results above, the errors are no longer dominated by the uncertainties in the input used for the electromagnetic corrections, though these are still significant at the level of precision reached in the  $N_f = 2 + 1$  results. This is due to the reduction in the error on  $\epsilon$  discussed in Sec. 3.1.1. Nevertheless, the comparison of Eqs. (28) and (30) indicates that more than half of the difference between the prediction  $m_u/m_d = 0.558$  obtained from Weinberg's mass formulae [88] and the result for  $m_u/m_d$  obtained on the lattice stems from electromagnetism, the higher orders in the chiral perturbation generating a comparable correction.

In view of the fact that a *massless up-quark* would solve the strong CP-problem, many authors have considered this an attractive possibility, but the results presented above exclude this possibility: the value of  $m_u$  in Eq. (30) differs from zero by 20 standard deviations. We conclude that nature solves the strong CP-problem differently. This conclusion relies on lattice calculations of kaon masses and on the phenomenological estimates of the e.m. self-energies discussed in Sec. 3.1.1. The uncertainties therein currently represent the limiting factor in determinations of  $m_u$  and  $m_d$ . As demonstrated in Refs. [20–22, 29–35, 37, 43], lattice methods can be used to calculate the e.m. self-energies. Further progress on the determination of the light-quark masses hinges on an improved understanding of the e.m. effects.

### 3.1.6 Estimates for $R$ and $Q$

The quark-mass ratios

$$R \equiv \frac{m_s - m_{ud}}{m_d - m_u} \quad \text{and} \quad Q^2 \equiv \frac{m_s^2 - m_{ud}^2}{m_d^2 - m_u^2} \quad (32)$$

compare  $SU(3)$  breaking with isospin breaking. The quantity  $Q$  is of particular interest because of a low-energy theorem [94], which relates it to a ratio of meson masses,

$$Q_M^2 \equiv \frac{\hat{M}_K^2}{\hat{M}_\pi^2} \cdot \frac{\hat{M}_K^2 - \hat{M}_\pi^2}{\hat{M}_{K^0}^2 - \hat{M}_{K^+}^2}, \quad \hat{M}_\pi^2 \equiv \frac{1}{2}(\hat{M}_{\pi^+}^2 + \hat{M}_{\pi^0}^2), \quad \hat{M}_K^2 \equiv \frac{1}{2}(\hat{M}_{K^+}^2 + \hat{M}_{K^0}^2). \quad (33)$$

Chiral symmetry implies that the expansion of  $Q_M^2$  in powers of the quark masses (i) starts with  $Q^2$  and (ii) does not receive any contributions at NLO:

$$Q_M \stackrel{\text{NLO}}{=} Q. \quad (34)$$

Inserting the estimates for the mass ratios  $m_s/m_{ud}$ , and  $m_u/m_d$  given for  $N_f = 2$  in Eqs. (17) and (29) respectively, we obtain

$$R = 40.7(3.7)(2.2), \quad Q = 24.3(1.4)(0.6), \quad (35)$$

where the errors have been propagated naively and the e.m. uncertainty has been separated out, as discussed in the third paragraph after Eq. (28). Thus, the meaning of the errors is the same as in Eq. (30). These numbers agree within errors with those reported in Ref. [37] where values for  $m_s$  and  $m_{ud}$  are taken from ETM 10B [54].

For  $N_f = 2 + 1$ , we use Eqs. (24) and (30) and obtain

$$R = 35.7(1.9)(1.8), \quad Q = 22.5(6)(6), \quad (36)$$

where the meaning of the errors is the same as above. The  $N_f = 2$  and  $N_f = 2 + 1$  results are compatible within  $2\sigma$ , even taking the correlations between e.m. effects into account.

Again, for  $N_f = 2 + 1 + 1$ , we simply take values from ETM 14A,

$$R = 35.6(5.1), \quad Q = 22.2(1.6), \quad (37)$$

which are quite compatible with two and three flavour results.

It is interesting to use these results to study the size of chiral corrections in the relations of  $R$  and  $Q$  to their expressions in terms of meson masses. To investigate this issue, we use  $\chi$ PT to express the quark-mass ratios in terms of the pion and kaon masses in QCD and then again use Eqs. (10)–(12) to relate the QCD masses to the physical ones. Linearizing in the corrections, this leads to

$$R \stackrel{\text{LO}}{=} R_M = 43.9 - 10.8 \epsilon + 0.2 \epsilon_{\pi^0} - 0.2 \epsilon_{K^0} - 10.7 \epsilon_m, \quad (38)$$

$$Q \stackrel{\text{NLO}}{=} Q_M = 24.3 - 3.0 \epsilon + 0.9 \epsilon_{\pi^0} - 0.1 \epsilon_{K^0} + 2.6 \epsilon_m. \quad (39)$$

While the first relation only holds to LO of the chiral perturbation series, the second remains valid at NLO, on account of the low-energy theorem mentioned above. The first terms on

the right hand side represent the values of  $R$  and  $Q$  obtained with the Weinberg leading-order formulae for the quark-mass ratios [88]. Inserting the estimates (13), we find that the e.m. corrections lower the Weinberg values to  $R_M = 36.7(3.3)$  and  $Q_M = 22.3(9)$ , respectively.

Comparison of  $R_M$  and  $Q_M$  with the full results quoted above gives a handle on higher-order terms in the chiral expansion. Indeed, the ratios  $R_M/R$  and  $Q_M/Q$  give NLO and NNLO (and higher)-corrections to the relations  $R \stackrel{\text{LO}}{=} R_M$  and  $Q \stackrel{\text{NLO}}{=} Q_M$ , respectively. The uncertainties due to the use of the e.m. corrections of Eq. (13) are highly correlated in the numerators and denominators of these ratios, and we make the simplifying assumption that they cancel in the ratio. Thus, for  $N_f = 2$  we evaluate Eqs. (38) and (39) using  $\epsilon = 0.79(18)(18)$  from RM123 13 [37] and the other corrections from Eq. (13), dropping all uncertainties. We divide them by the results for  $R$  and  $Q$  in Eq. (35), omitting the uncertainties due to e.m. We obtain  $R_M/R \simeq 0.88(8)$  and  $Q_M/Q \simeq 0.91(5)$ . We proceed analogously for  $N_f = 2 + 1$  and  $2+1+1$ , using  $\epsilon = 0.70(3)$  from Eq. (13) and  $R$  and  $Q$  from Eqs. (36) and (37), and find  $R_M/R \simeq 1.02(5)$  and  $1.03(17)$ , and  $Q_M/Q \simeq 0.99(3)$  and  $1.00(8)$ . The chiral corrections appear to be small for three and four flavours, especially those in the relation of  $Q$  to  $Q_M$ . This is less true for  $N_f = 2$ , where the NNLO and higher corrections to  $Q = Q_M$  could be significant. However, as for other quantities which depend on  $m_u/m_d$ , this difference is not significant.

As mentioned in Sec. 3.1.1, there is a phenomenological determination of  $Q$  based on the decay  $\eta \rightarrow 3\pi$  [95, 96]. The key point is that the transition  $\eta \rightarrow 3\pi$  violates isospin conservation. The dominating contribution to the transition amplitude stems from the mass difference  $m_u - m_d$ . At NLO of  $\chi$ PT, the QCD part of the amplitude can be expressed in a parameter-free manner in terms of  $Q$ . It is well-known that the electromagnetic contributions to the transition amplitude are suppressed (a thorough recent analysis is given in Ref. [97]). This implies that the result for  $Q$  is less sensitive to the electromagnetic uncertainties than the value obtained from the masses of the Nambu-Goldstone bosons. For a recent update of this determination and for further references to the literature, we refer to Ref. [98]. Using dispersion theory to pin down the momentum dependence of the amplitude, the observed decay rate implies  $Q = 22.3(8)$  (since the uncertainty quoted in Ref. [98] does not include an estimate for all sources of error, we have retained the error estimate given in Ref. [91], which is twice as large). The formulae for the corrections of NNLO are available also in this case [99] – the poor knowledge of the effective coupling constants, particularly of those that are relevant for the dependence on the quark masses, is currently the limiting factor encountered in the application of these formulae.

As was to be expected, the central value of  $Q$  obtained from  $\eta$ -decay agrees exactly with the central value obtained from the low-energy theorem: we have used that theorem to estimate the coefficient  $\epsilon$ , which dominates the e.m. corrections. Using the numbers for  $\epsilon_m$ ,  $\epsilon_{\pi^0}$  and  $\epsilon_{K^0}$  in Eq. (13) and adding the corresponding uncertainties in quadrature to those in the phenomenological result for  $Q$ , we obtain

$$\epsilon \stackrel{\text{NLO}}{=} 0.70(28). \quad (40)$$

The estimate (13) for the size of the coefficient  $\epsilon$  is taken from here, as it is confirmed by the most recent, preliminary lattice determinations [29–31, 34, 35, 37].

Our final results for the masses  $m_u$ ,  $m_d$ ,  $m_{ud}$ ,  $m_s$  and the mass ratios  $m_u/m_d$ ,  $m_s/m_{ud}$ ,  $R$ ,  $Q$  are collected in Tabs. 8 and 9. We separate  $m_u$ ,  $m_d$ ,  $m_u/m_d$ ,  $R$  and  $Q$  from  $m_{ud}$ ,  $m_s$  and  $m_s/m_{ud}$ , because the latter are completely dominated by lattice results while the former



still include some phenomenological input.

$N_f$	$m_{ud}$	$m_s$	$m_s/m_{ud}$
2+1+1	3.70(17)	93.9(1.1)	27.30(34)
2+1	3.373(80)	92.0(2.1)	27.43(31)
2	3.6(2)	101(3)	27.3(9)

Table 8: Our estimates for the strange-quark and the average up-down-quark masses in the  $\overline{\text{MS}}$  scheme at running scale  $\mu = 2 \text{ GeV}$ . Numerical values are given in MeV. In the results presented here, the error is the one which we obtain by applying the averaging procedure of Sec. 2.3 to the relevant lattice results. We have added an uncertainty to the  $N_f = 2 + 1$  results, associated with the neglect of the charm sea-quark and isospin-breaking effects, as discussed around Eqs. (18) and (24). This uncertainty is not included in the  $N_f = 2$  results, as it should be smaller than the uncontrolled systematic associated with the neglect of strange sea-quark effects.

$N_f$	$m_u$	$m_d$	$m_u/m_d$	$R$	$Q$
2+1+1	2.36(24)	5.03(26)	0.470(56)	35.6(5.1)	22.2 (1.6)
2+1	2.16(9)(7)	4.68(14)(7)	0.46(2)(2)	35.0(1.9)(1.8)	22.5(6)(6)
2	2.40(23)	4.80(23)	0.50(4)	40.7(3.7)(2.2)	24.3(1.4)(0.6)

Table 9: Our estimates for the masses of the two lightest quarks and related, strong isospin-breaking ratios. Again, the masses refer to the  $\overline{\text{MS}}$  scheme at running scale  $\mu = 2 \text{ GeV}$ . Numerical values are given in MeV. In the results presented here, the first error is the one that comes from lattice computations while the second for  $N_f = 2 + 1$  is associated with the phenomenological estimate of e.m. contributions, as discussed after Eq. (30). The second error on the  $N_f = 2$  results for  $R$  and  $Q$  is also an estimate of the e.m. uncertainty, this time associated with the lattice computation of Ref. [37], as explained after Eq. (35). We present these results in a separate table, because they are less firmly established than those in Tab. 8. For  $N_f = 2 + 1$  and 2+1+1 they still include information coming from phenomenology, in particular on e.m. corrections, and for  $N_f = 2$  the e.m. contributions are computed neglecting the feedback of sea quarks on the photon field.

### 3.2 Charm-quark mass

In the present review we collect and discuss for the first time the lattice determinations of the  $\overline{\text{MS}}$  charm-quark mass  $\overline{m}_c$ . Most of the results have been obtained by analyzing the lattice-QCD simulations of 2-point heavy-light- or heavy-heavy-meson correlation functions, using as input the experimental values of the  $D$ ,  $D_s$  and charmonium mesons. The exceptions

are represented by the HPQCD 14A [11] result at  $N_f = 2 + 1 + 1$ , the HPQCD 08B [79], HPQCD 10 [66] and JLQCD 15B [100] results at  $N_f = 2 + 1$ , and the ETM 11F [101] result at  $N_f = 2$ , where the moments method has been employed. The latter is based on the lattice calculation of the Euclidean time moments of pseudoscalar-pseudoscalar correlators for heavy-quark currents followed by an OPE expansion dominated by perturbative QCD effects, which provides the determination of both the heavy-quark mass and the strong coupling constant  $\alpha_s$ .

The heavy-quark actions adopted by the various lattice collaborations have been reviewed already in the FLAG 13 review [2], and their descriptions can be found in Sec. A.1.3. While the charm mass determined with the moments method does not need any lattice evaluation of the mass renormalization constant  $Z_m$ , the extraction of  $\bar{m}_c$  from 2-point heavy-meson correlators does require the nonperturbative calculation of  $Z_m$ . The lattice scale at which  $Z_m$  is obtained, is usually at least of the order 2–3 GeV, and therefore it is natural in this review to provide the values of  $\bar{m}_c(\mu)$  at the renormalization scale  $\mu = 3$  GeV. Since the choice of a renormalization scale equal to  $\bar{m}_c$  is still commonly adopted (as by PDG [78]), we have collected in Tab. 10 the lattice results for both  $\bar{m}_c(\bar{m}_c)$  and  $\bar{m}_c(3 \text{ GeV})$ , obtained at  $N_f = 2$ ,  $2 + 1$  and  $2 + 1 + 1$ . When not directly available in the publications, we apply a conversion factor equal either to 0.900 between the scales  $\mu = 2$  GeV and  $\mu = 3$  GeV or to 0.766 between the scales  $\mu = \bar{m}_c$  and  $\mu = 3$  GeV, obtained using perturbative QCD evolution at four loops assuming  $\Lambda_{QCD} = 300$  MeV for  $N_f = 4$ .

In the next subsections we review separately the results of  $\bar{m}_c(\bar{m}_c)$  for the various values of  $N_f$ .

### 3.2.1 $N_f = 2 + 1 + 1$ results

There are three recent results employing four dynamical quarks in the sea. ETM 14 [9] uses 15 twisted mass gauge ensembles at 3 lattice spacings ranging from 0.062 to 0.089 fm (using  $f_\pi$  as input), in boxes of size ranging from 2.0 to 3.0 fm and pion masses from 210 to 440 MeV (explaining the tag  $\circ$  in the chiral extrapolation and the tag  $\star$  for the continuum extrapolation). The value of  $M_\pi L$  at their smallest pion mass is 3.2 with more than two volumes (explaining the tag  $\circ$  in the finite-volume effects). They fix the strange mass with the kaon mass and the charm one with that of the  $D_s$  and  $D$  mesons.

ETM 14A [102] uses 10 out of the 15 gauge ensembles adopted in ETM 14 spanning the same range of values for the pion mass and the lattice spacing, but the latter is fixed using the nucleon mass. Two lattice volumes with size larger than 2.0 fm are employed. The physical strange and the charm mass are obtained using the masses of the  $\Omega^-$  and  $\Lambda_c^+$  baryons, respectively.

HPQCD 14A [11] works with the moments method adopting HISQ staggered fermions. Their results are based on 9 out of the 21 ensembles carried out by the MILC collaboration [10] at 4 values of the coupling  $\beta$  corresponding to lattice spacings in the range from 0.057 to 0.153 fm, in boxes of sizes up to 5.8 fm and with taste-Goldstone-pion masses down to 130 MeV and RMS-pion masses down to 173 MeV. The strange- and charm-quark masses are fixed using as input the lattice result  $M_{\bar{s}s} = 688.5(2.2)$  MeV, calculated without including  $\bar{s}s$  annihilation effects, and  $M_{\eta_c} = 2.9863(27)$  GeV, obtained from the experimental  $\eta_c$  mass after correcting for  $\bar{c}c$  annihilation and e.m. effects. All of the selection criteria of Sec. 2.1.1 are satisfied with the tag  $\star$ <sup>4</sup>.

<sup>4</sup>Note that in Section 9.7.2 different coding criteria are adopted and the HPQCD 14A paper is tagged

Collaboration	Ref.	$N_f$	publication status	chiral extrapolation	continuum extrapolation	finite volume	renormalization	$\overline{m}_c(\overline{m}_c)$	$\overline{m}_c(3 \text{ GeV})$
HPQCD 14A	[11]	2+1+1	A	★	★	★	–	1.2715(95)	0.9851(63)
ETM 14A	[102]	2+1+1	A	○	★	○	★	1.3478(27)(195)	1.0557(22)(153)
ETM 14	[9]	2+1+1	A	○	★	○	★	1.348(46)	1.058(35)
JLQCD 15B	[100]	2+1	C	○	★	★	–	1.2769(21)(89)	0.9948(16)(69)
$\chi$ QCD 14	[103]	2+1	A	○	○	○	★	1.304(5)(20)	1.006(5)(22)
HPQCD 10	[66]	2+1	A	○	★	○	–	1.273(6)	0.986(6)
HPQCD 08B	[79]	2+1	A	○	★	○	–	1.268(9)	0.986(10)
ALPHA 13B	[104]	2	C	★	○	★	★	1.274(36)	0.976(28)
ETM 11F	[101]	2	C	○	★	○	–	1.279(12)/1.296(18)*	0.979(09)/0.998(14)*
ETM 10B	[54]	2	A	○	★	○	★	1.28(4)	1.03(4)
PDG	[78]							1.275(25)	

\* Two results are quoted.

Table 10: Lattice results for the  $\overline{\text{MS}}$ -charm-quark mass  $\overline{m}_c(\overline{m}_c)$  and  $\overline{m}_c(3 \text{ GeV})$  in GeV, together with the colour coding of the calculations used to obtain these. When not directly available in the publications, a conversion factor equal to 0.900 between the scales  $\mu = 2 \text{ GeV}$  and  $\mu = 3 \text{ GeV}$  (or equal to 0.766 between the scales  $\mu = \overline{m}_c$  and  $\mu = 3 \text{ GeV}$ ) has been considered.

According to our rules on the publication status all the three results can enter the FLAG average at  $N_f = 2 + 1 + 1$ . The determinations of  $\overline{m}_c$  obtained by ETM 14 and 14A agree quite well with each other, but they are not compatible with the HPQCD 14A result. Therefore we first combine the two ETM results with a 100% correlation in the statistical error, yielding  $\overline{m}_c(\overline{m}_c) = 1.348(20)\text{GeV}$ . Then we perform the average with the HPQCD 14A result, obtaining the final FLAG averages

$$N_f = 2 + 1 + 1: \quad \overline{m}_c(\overline{m}_c) = 1.286(30) \text{ GeV} \quad \text{Refs. [9, 11]}, \quad (41)$$

$$\overline{m}_c(3 \text{ GeV}) = 0.996(25) \text{ GeV} \quad \text{Refs. [9, 11]}, \quad (42)$$

where the errors include a quite large value (3.5 and 4.4, respectively) for the stretching factor  $\sqrt{\chi^2/\text{dof}}$  coming from our rules for the averages discussed in Sec. 2.2.

### 3.2.2 $N_f = 2 + 1$ results

The HPQCD 10 [66] result is based on the moments method adopting a subset of  $N_f = 2 + 1$  Asqtad-staggered-fermion ensembles from MILC [25], on which HISQ valence fermions are differently for the continuum extrapolation.

studied. The charm mass is fixed from that of the  $\eta_c$  meson,  $M_{\eta_c} = 2.9852(34)$  GeV corrected for  $\bar{c}c$  annihilation and e.m. effects. HPQCD 10 replaces the result HPQCD 08B [79], in which Asqtad staggered fermions have been used also for the valence quarks.

$\chi$ QCD 14 [103] uses a mixed-action approach based on overlap fermions for the valence quarks and on domain-wall fermions for the sea quarks. They adopt six of the gauge ensembles generated by the RBC/UKQCD collaboration [70] at two values of the lattice spacing (0.087 and 0.11 fm) with unitary pion masses in the range from 290 to 420 MeV. For the valence quarks no light-quark masses are simulated. At the lightest pion mass  $M_\pi \simeq 290$  MeV, the value of  $M_\pi L$  is 4.1, which satisfies the tag  $\circ$  for the finite-volume effects. The strange- and charm-quark masses are fixed together with the lattice scale by using the experimental values of the  $D_s$ ,  $D_s^*$  and  $J/\psi$  meson masses.

JLQCD 15B [100] determines the charm mass through the moments method using Möbius domain-wall fermions at three values of the lattice spacing, ranging from 0.044 to 0.083 fm. The lightest pion mass is  $\simeq 230$  MeV and the corresponding value of  $M_\pi L$  is  $\simeq 4.4$ .

Thus, according to our rules on the publication status, the FLAG average for the charm-quark mass at  $N_f = 2 + 1$  is obtained by combining the two results HPQCD 10 and  $\chi$ QCD 14, leading to

$$N_f = 2 + 1: \quad \bar{m}_c(\bar{m}_c) = 1.275 (8) \text{ GeV} \quad \text{Refs. [66, 103],} \quad (43)$$

$$\bar{m}_c(3 \text{ GeV}) = 0.987 (6) \text{ GeV} \quad \text{Refs. [66, 103],} \quad (44)$$

where the error on  $\bar{m}_c(\bar{m}_c)$  includes a stretching factor  $\sqrt{\chi^2/\text{dof}} \simeq 1.4$  as discussed in Sec. 2.2.

### 3.2.3 $N_f = 2$ results

We turn now to the three results at  $N_f = 2$ .

ETM 10B [54] is based on tmQCD simulations at four values of the lattice spacing in the range from 0.05 fm to 0.1 fm, with pion masses as low as 270 MeV at two lattice volumes. They fix the strange-quark mass with either  $M_K$  or  $M_{\bar{s}s}$  and the charm mass using alternatively the  $D$ ,  $D_s$  and  $\eta_c$  masses.

ETM 11F [101] is based on the same gauge ensemble as ETM 10B, but the moments method is adopted.

ALPHA 13B uses a subset of the CLS gauge ensembles with  $\mathcal{O}(a)$ -improved Wilson fermions generated at two values of the lattice spacing (0.048 fm and 0.065 fm), using the kaon decay constant to fix the scale. The pion masses are as low as 190 MeV with the value of  $M_\pi L$  equal to  $\simeq 4$  at the lightest pion mass (explaining the tag  $\star$  for finite-volume effects).

According to our rules on the publication status ETM 10B becomes the FLAG average at  $N_f = 2$ , n-mely

$$N_f = 2: \quad \bar{m}_c(\bar{m}_c) = 1.28 (4) \text{ GeV} \quad \text{Ref. [54],} \quad (45)$$

$$\bar{m}_c(3 \text{ GeV}) = 1.03 (4) \text{ GeV} \quad \text{Ref. [54].} \quad (46)$$

In Fig. 4 the lattice results of Tab. 10 and the FLAG averages obtained at  $N_f = 2$ ,  $2 + 1$  and  $2 + 1 + 1$  are presented.

### 3.2.4 Lattice determinations of the ratio $m_c/m_s$

Because some of the results for the light-quark masses given in this review are obtained via the quark-mass ratio  $m_c/m_s$ , we now review also these lattice calculations, which are listed

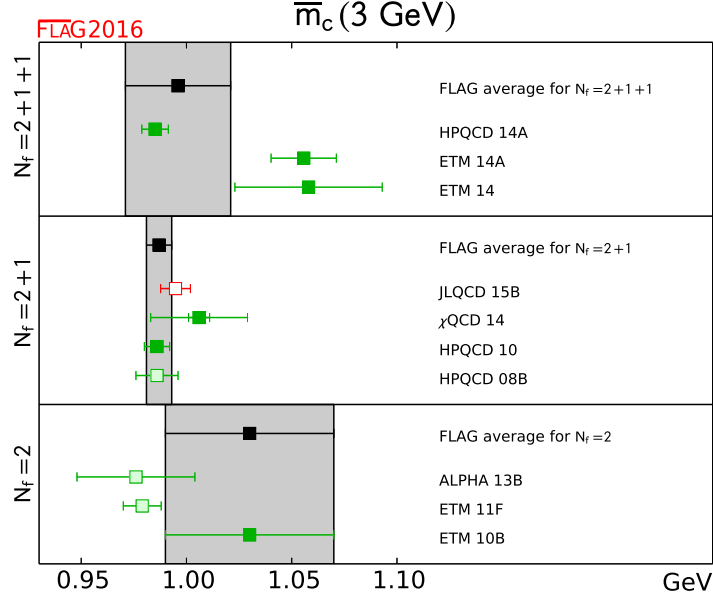


Figure 4: Lattice results and FLAG averages at  $N_f = 2, 2+1,$  and  $2+1+1$  for the charm-quark mass  $\bar{m}_c(3 \text{ GeV})$ .

in Tab. 11.

Collaboration	Ref.	$N_f$	Publication status	chiral extrapolation	continuum extrapolation	finite volume	$m_c/m_s$
HPQCD 14A	[11]	2+1+1	A	★	★	★	11.652(35)(55)
FNAL/MILC 14A	[10]	2+1+1	A	★	★	★	11.747(19)( $^{+59}_{-43}$ )
ETM 14	[9]	2+1+1	A	○	★	○	11.62(16)
$\chi$ QCD 14	[103]	2+1	A	○	○	○	11.1(8)
HPQCD 09A	[71]	2+1	A	○	★	★	11.85(16)
ETM 14D	[87]	2	C	★	■	■	12.29(10)
Dürr 11	[55]	2	A	○	★	○	11.27(30)(26)
ETM 10B	[54]	2	A	○	★	○	12.0(3)

Table 11: Lattice results for the quark-mass ratio  $m_c/m_s$ , together with the colour coding of the calculations used to obtain these.

We begin with the  $N_f = 2$  results. Besides the result ETM 10B, already discussed in Sec. 3.2.3, there are two more results, Dürr 11 [55] and ETM 14D [87]. Dürr 11 [55] is based

on QCDSF  $N_f = 2$   $\mathcal{O}(a)$ -improved Wilson-fermion simulations [62, 105] on which valence, Brillouin-improved Wilson quarks [106] are considered. It features only 2 ensembles with  $M_\pi < 400$  MeV. The bare axial-Ward-identity (AWI) masses for  $m_s$  and  $m_c$  are tuned to simultaneously reproduce the physical values of  $M_{\bar{s}s}^2/(M_{D_s^*}^2 - M_{D_s}^2)$  and  $(2M_{D_s^*}^2 - M_{\bar{s}s}^2)/(M_{D_s^*}^2 - M_{D_s}^2)$ , where  $M_{\bar{s}s}^2 = 685.8(8)$  MeV is the quark-connected- $\bar{s}s$  pseudoscalar mass.

The ETM 14D result [87] is based on recent ETM gauge ensembles generated close to the physical point with the addition of a clover term to the tmQCD action. The new simulations are performed at a single lattice spacing of  $\simeq 0.09$  fm and at a single box size  $L \simeq 4$  fm and therefore their calculations do not pass our criteria for the continuum extrapolation and finite-volume effects. The FLAG average at  $N_f = 2$  can be therefore obtained by averaging ETM 10B and Dürre 11, obtaining

$$N_f = 2: \quad m_c/m_s = 11.74 \quad (35) \quad \text{Ref. [54, 55]}, \quad (47)$$

where the error includes the stretching factor  $\sqrt{\chi^2/\text{dof}} \simeq 1.5$ .

The situation is similar also for the  $N_f = 2 + 1$  results, as besides  $\chi$ QCD 14 there is only the result HPQCD 09A [71]. The latter is based on a subset of  $N_f = 2 + 1$  Asqtad-staggered-fermion simulations from MILC, on which HISQ-valence fermions are studied. The strange mass is fixed with  $M_{\bar{s}s} = 685.8(4.0)$ , MeV and the charm's from that of the  $\eta_c$ ,  $M_{\eta_c} = 2.9852(34)$  GeV corrected for  $\bar{c}c$  annihilation and e.m. effects. By combing the results  $\chi$ QCD 14 and HPQCD 09A we obtain

$$N_f = 2 + 1: \quad m_c/m_s = 11.82 \quad (16) \quad \text{Refs. [71, 103]}, \quad (48)$$

with a  $\chi^2/\text{dof} \simeq 0.85$ .

Turning now to the  $N_f = 2 + 1 + 1$  results, in addition to the HPQCD 14A and ETM 14 calculations, already described in Sec. 3.2.1, we consider the recent FNAL/MILC 14 result [10], where HISQ staggered fermions are employed. Their result is based on the use of 21 gauge ensembles at 4 values of the coupling  $\beta$  corresponding to lattice spacings in the range from 0.057 to 0.153 fm, in boxes of sizes up to 5.8 fm and with taste-Goldstone-pion masses down to 130 MeV and RMS-pion masses down to 143 MeV. They fix the strange mass with  $M_{\bar{s}s}$ , corrected for e.m. effects with  $\bar{\epsilon} = 0.84(20)$  [32]. The charm mass is fixed with the mass of the  $D_s$  meson. As for the HPQCD 14A result, all of our selection criteria are satisfied with the tag  $\star$ . However a slight tension exists between the two results. Indeed by combining HPQCD 14A and FNAL/MILC 14 results, assuming a 100 % correlation between the statistical errors (since the two results share the same gauge configurations), we obtain  $m_c/m_s = 11.71(6)$ , where the error includes the stretching factor  $\sqrt{\chi^2/\text{dof}} \simeq 1.35$ . A further average with the ETM 14A result leads to our final average

$$N_f = 2 + 1 + 1: \quad m_c/m_s = 11.70 \quad (6) \quad \text{Refs. [9–11]}, \quad (49)$$

which has a remarkable overall precision of 0.5 %.

All of the results for  $m_c/m_s$  discussed above are shown in Fig. 5 together with the FLAG averages corresponding to  $N_f = 2, 2 + 1$  and  $2 + 1 + 1$ .

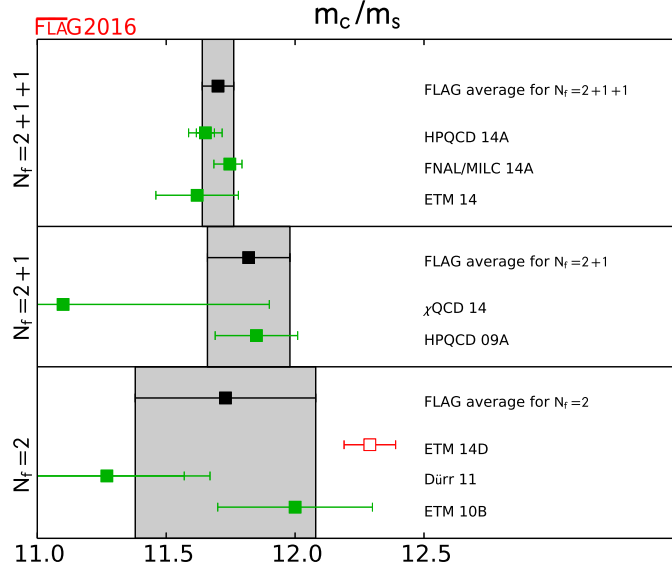


Figure 5: Lattice results for the ratio  $m_c/m_s$  listed in Tab. 11 and the FLAG averages corresponding to  $N_f = 2, 2 + 1$  and  $2 + 1 + 1$ .

### 3.3 Bottom-quark mass

We now give the lattice results for the  $\overline{\text{MS}}$ -bottom-quark mass  $\overline{m}_b$  for the first time as part of this review. Related heavy-quark actions and observables have been discussed in the FLAG 13 review [2], and descriptions can be found in Sec. A.1.3. In Tab. 12 we have collected the lattice results for  $\overline{m}_b(\overline{m}_b)$  obtained at  $N_f = 2, 2 + 1$  and  $2 + 1 + 1$ , which in the following we review separately. Available results for the quark-mass ratio  $m_b/m_c$  are also reported. Afterwards we evaluate the corresponding FLAG averages.

#### 3.3.1 $N_f = 2 + 1 + 1$

Results have been published by HPQCD using NRQCD and HISQ-quark actions (HPQCD 14B [107] and HPQCD 14A [11], respectively). In both works the  $b$ -quark mass is computed with the moments method, that is, from Euclidean-time moments of two-point, heavy-heavy meson correlation functions (see Sec. 9.7 for a description of the method).

In HPQCD 14B the  $b$ -quark mass is computed from ratios of the moments  $R_n$  of heavy current-current correlation functions, namely

$$\left[ \frac{R_n r_{n-2}}{R_{n-2} r_n} \right]^{1/2} \frac{\overline{M}_{\text{kin}}}{2m_b} = \frac{\overline{M}_{\Upsilon, \eta_b}}{2\overline{m}_b(\mu)}, \quad (50)$$

where  $r_n$  are the perturbative moments calculated at  $\text{N}^3\text{LO}$ ,  $\overline{M}_{\text{kin}}$  is the spin-averaged kinetic mass of the heavy-heavy vector and pseudoscalar mesons and  $\overline{M}_{\Upsilon, \eta_b}$  is the experimental spin average of the  $\Upsilon$  and  $\eta_b$  masses. The kinetic mass  $\overline{M}_{\text{kin}}$  is chosen since in the lattice calculation

Collaboration	Ref.	$N_f$	publication status	chiral extrapolation	continuum extrapolation	finite volume	renormalization	heavy quark treatment	$\bar{m}_b(\bar{m}_b)$	$m_b/m_c$
HPQCD 14B	[107]	2+1+1	A	★	★	★	★	✓	4.196(23) <sup>†</sup>	
ETM 14B	[108]	2+1+1	C	○	★	○	★	✓	4.26(7)(14)	4.40(6)(5)
HPQCD 14A	[11]	2+1+1	A	★	★	★	–	✓	4.162(48)	4.528(14)(52)
HPQCD 13B	[109]	2+1	A	■	○	–	–	✓	4.166(43)	
HPQCD 10	[66]	2+1	A	★	★	★	–	✓	4.164(23) <sup>*</sup>	4.51(4)
ETM 13B	[110]	2	A	○	★	○	★	✓	4.31(9)(8)	
ALPHA 13C	[111]	2	A	★	★	★	★	✓	4.21(11)	
ETM 11A	[112]	2	A	○	★	○	★	✓	4.29(14)	
PDG	[78]								4.18(3)	

<sup>†</sup> Warning: only two pion points are used for chiral extrapolation.

<sup>\*</sup> The number that is given is  $m_b(10 \text{ GeV}, N_f = 5) = 3.617(25) \text{ GeV}$ .

Table 12: Lattice results for the  $\overline{\text{MS}}$ -bottom-quark mass  $\bar{m}_b(\bar{m}_b)$  in GeV, together with the systematic error ratings for each. Available results for the quark mass ratio  $m_b/m_c$  are also reported.

the splitting of the  $\Upsilon$  and  $\eta_b$  states is inverted. In Eq. (50) the bare mass  $m_b$  appearing on the left hand side is tuned so that the spin-averaged mass agrees with experiment, while the mass  $\bar{m}_b$  at the fixed scale  $\mu = 4.18 \text{ GeV}$  is extrapolated to the continuum limit using three HISQ (MILC) ensembles with  $a \approx 0.15, 0.12$  and  $0.09 \text{ fm}$  and two pion masses, one of which is the physical one. Therefore according to our rules on the chiral extrapolation a warning must be given. Their final result is  $\bar{m}_b(\mu = 4.18 \text{ GeV}) = 4.207(26) \text{ GeV}$ , where the error is from adding systematic uncertainties in quadrature only (statistical errors are smaller than 0.1% and ignored). The errors arise from renormalization, perturbation theory, lattice spacing, and NRQCD systematics. The finite-volume uncertainty is not estimated, but at the lowest pion mass they have  $m_\pi L \simeq 4$ , which leads to the tag ★.

In HPQCD 14A the quark mass is computed using a similar strategy as above but with HISQ heavy quarks instead of NRQCD. The gauge-field ensembles are the same as in HPQCD 14B above plus the one with  $a = 0.06 \text{ fm}$  (four lattice spacings in all). Bare heavy-quark masses are tuned to their physical values using the  $\eta_h$  mesons, and ratios of ratios yield  $m_h/m_c$ . The  $\overline{\text{MS}}$ -charm-quark mass determined as described in Sec. 3.2 then gives  $m_b$ . The moment ratios are expanded using the OPE, and the quark masses and  $\alpha_S$  are determined from fits of the lattice ratios to this expansion. The fits are complicated: HPQCD uses cubic splines for valence- and sea-mass dependence, with several knots, and many priors for 21 ratios to fit 29 data points. Taking this fit at face value results in a ★ rating for the continuum



limit since they use four lattice spacings down to 0.06 fm. See however the detailed discussion of the continuum limit given in Sec. 9.7 on  $\alpha_S$ .

The third four-flavour result is from the ETM Collaboration and appears in a conference proceedings, so it is not included in our final average. The calculation is performed on a set of configurations generated with twisted Wilson fermions with three lattice spacings in the range 0.06 to 0.09 fm and with pion masses in the range 210 to 440 MeV. The  $b$ -quark mass is determined from a ratio of heavy-light pseudoscalar meson masses designed to yield the quark pole mass in the static limit. The pole mass is related to the  $\overline{\text{MS}}$  mass through perturbation theory at N<sup>3</sup>LO. The key idea is that by taking ratios of ratios, the  $b$ -quark mass is accessible through fits to heavy-light(strange)-meson correlation functions computed on the lattice in the range  $\sim 1 - 2 \times m_c$  and the static limit, the latter being exactly 1. By simulating below  $\overline{m}_b$ , taking the continuum limit is easier. They find  $\overline{m}_b(\overline{m}_b) = 4.26(7)(14)$  GeV, where the first error is statistical and the second systematic. The dominant errors come from setting the lattice scale and fit systematics.

### 3.3.2 $N_f = 2 + 1$

HPQCD 13B [109] extracts  $\overline{m}_b$  from a lattice determination of the  $\Upsilon$  energy in NRQCD and the experimental value of the meson mass. The latter quantities yield the pole mass which is related to the  $\overline{\text{MS}}$  mass in 3-loop perturbation theory. The MILC coarse (0.12 fm) and fine (0.09 fm) Asqtad-2+1-flavour ensembles are employed in the calculation. The bare light-(sea)-quark masses correspond to a single, relatively heavy, pion mass of about 300 MeV. No estimate of the finite-volume error is given.

The value of  $\overline{m}_b(\overline{m}_b)$  reported in HPQCD 10 [66] is computed in a very similar fashion to the one in HPQCD 14A described in the last section, except that MILC 2+1-flavour-Asqtad ensembles are used under HISQ-heavy-valence quarks. The lattice spacings of the ensembles range from 0.18 to 0.045 fm and pion masses down to about 165 MeV. In all, 22 ensembles were fit simultaneously. An estimate of the finite-volume error based on leading-order perturbation theory for the moment ratio is also provided. Details of perturbation theory and renormalization systematics are given in Sec. 9.7.

### 3.3.3 $N_f = 2$

The ETM Collaboration computes  $\overline{m}_b(\overline{m}_b)$  using the ratio method described above on two-flavour twisted-mass gauge ensembles with four values of the lattice spacing in the range 0.10 to 0.05 fm and pion masses between 280 and 500 MeV (ETM 13B updates ETM 11). The heavy-quark masses cover a range from charm to a little more than three GeV, plus the exact static-limit point. They find  $\overline{m}_b(\overline{m}_b) = 4.31(9)(8)$  GeV for two-flavour running, while  $\overline{m}_b(\overline{m}_b) = 4.27(9)(8)$  using four-flavour running, from the 3 GeV scale used in the N<sup>3</sup>LO perturbative matching calculation from the pole mass to the  $\overline{\text{MS}}$  mass. The latter are computed nonperturbatively in the RI-MOM scheme at 3 GeV and matched to  $\overline{\text{MS}}$ . The dominant errors are combined statistical+fit(continuum+chiral limits) and the uncertainty in setting the lattice scale. ETM quotes the average of two- and five-flavour results,  $\overline{m}_b(\overline{m}_b) = 4.29(9)(8)(2)$  where the last error is one-half the difference between the two. In our average (see below), we use the two-flavour result.

The Alpha Collaboration uses HQET for heavy-light mesons to obtain  $m_b$  [111] (ALPHA 13C). They employ CLS, nonperturbatively improved, Wilson gauge field ensembles with

three lattice spacings (0.075-0.048 fm), pion masses from 190 to 440 MeV, and three or four volumes at each lattice spacing, with  $m_\pi L > 4.0$ . The bare-quark mass is related to the RGI-scheme mass using the Schrödinger Functional technique with conversion to  $\overline{\text{MS}}$  through four-loop anomalous dimensions for the mass. The final result, extrapolated to the continuum and chiral limits, is  $\overline{m}_b(\overline{m}_b) = 4.21(11)$  with two-flavour running, where the error combines statistical and systematic uncertainties. The value includes all corrections in HQET through  $\Lambda^2/m_b$ , but repeating the calculation in the static limit yields the identical result, indicating the HQET expansion is under very good control.

### 3.3.4 Averages for $\overline{m}_b(\overline{m}_b)$

Taking the results that meet our rating criteria,  $\circ$ , or better, we compute the averages from HPQCD 14A and 14B for  $N_f = 2 + 1 + 1$ , ETM 13B and ALPHA 13C for  $N_f = 2$ , and we take HPQCD 10 as estimate for  $N_f = 2 + 1$ , obtaining

$$N_f = 2 + 1 + 1 : \quad \overline{m}_b(\overline{m}_b) = 4.190(21) \quad \text{Refs. [11, 107]}, \quad (51)$$

$$N_f = 2 + 1 : \quad \overline{m}_b(\overline{m}_b) = 4.164(23) \quad \text{Ref. [66]}, \quad (52)$$

$$N_f = 2 : \quad \overline{m}_b(\overline{m}_b) = 4.256(81) \quad \text{Refs. [110, 111]}. \quad (53)$$

Since HPQCD quotes  $\overline{m}_b(\overline{m}_b)$  values using  $N_f = 5$  running, we used those values directly in these  $N_f = 2 + 1 + 1$  and  $2+1$  averages. The results ETM 13B and ALPHA 13C, entering the average at  $N_f = 2$ , correspond to the  $N_f = 2$  running.

All the results for  $\overline{m}_b(\overline{m}_b)$  discussed above are shown in Fig. 6 together with the FLAG averages corresponding to  $N_f = 2, 2 + 1$  and  $2 + 1 + 1$ .

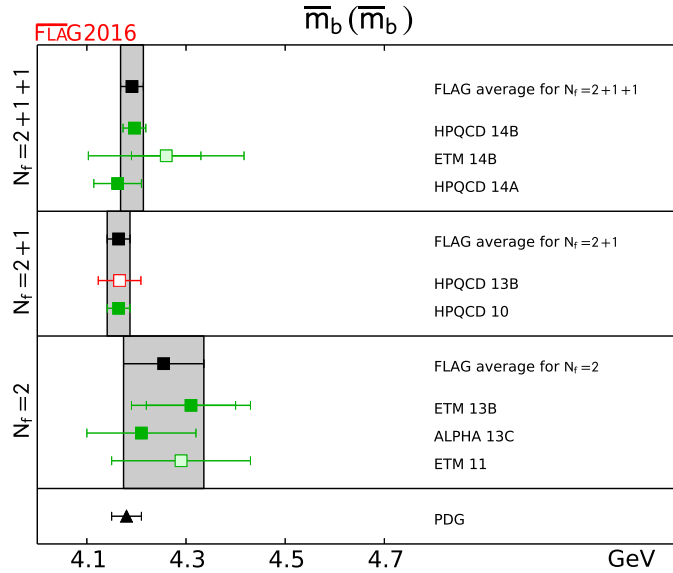


Figure 6: Lattice results and FLAG averages at  $N_f = 2, 2 + 1$ , and  $2 + 1 + 1$  for the  $b$ -quark mass  $\overline{m}_b(\overline{m}_b)$ . The updated PDG value from Ref. [78] is reported for comparison.

## References

- [1] A. Manohar and C. T. Sachrajda, *Quark masses*, in *Review of Particle Physics*, *Chin. Phys.* **C38** (2014) 090001.
- [2] [FLAG 13] S. Aoki, Y. Aoki, C. Bernard, T. Blum, G. Colangelo et al., *Review of lattice results concerning low-energy particle physics*, *Eur.Phys.J.* **C74** (2014) 2890, [[1310.8555](#)].
- [3] [PACS-CS 08] S. Aoki et al., *2+1 flavor lattice QCD toward the physical point*, *Phys. Rev.* **D79** (2009) 034503, [[0807.1661](#)].
- [4] [PACS-CS 09] S. Aoki et al., *Physical point simulation in 2+1 flavor lattice QCD*, *Phys. Rev.* **D81** (2010) 074503, [[0911.2561](#)].
- [5] [PACS-CS 10] S. Aoki et al., *Non-perturbative renormalization of quark mass in  $N_f = 2 + 1$  QCD with the Schrödinger functional scheme*, *JHEP* **1008** (2010) 101, [[1006.1164](#)].
- [6] [BMW 10A] S. Dürr, Z. Fodor, C. Hoelbling, S. Katz, S. Krieg et al., *Lattice QCD at the physical point: light quark masses*, *Phys.Lett.* **B701** (2011) 265–268, [[1011.2403](#)].
- [7] [BMW 10B] S. Dürr, Z. Fodor, C. Hoelbling, S. Katz, S. Krieg et al., *Lattice QCD at the physical point: simulation and analysis details*, *JHEP* **1108** (2011) 148, [[1011.2711](#)].
- [8] [RBC/UKQCD 12] R. Arthur et al., *Domain wall QCD with near-physical pions*, *Phys.Rev.* **D87** (2013) 094514, [[1208.4412](#)].
- [9] [ETM 14] N. Carrasco et al., *Up, down, strange and charm quark masses with  $N_f = 2+1+1$  twisted mass lattice QCD*, *Nucl. Phys.* **B887** (2014) 19–68, [[1403.4504](#)].
- [10] [FNAL/MILC 14A] A. Bazavov et al., *Charmed and light pseudoscalar meson decay constants from four-flavor lattice QCD with physical light quarks*, *Phys.Rev.* **D90** (2014) 074509, [[1407.3772](#)].
- [11] [HPQCD 14A] B. Chakraborty, C. T. H. Davies, G. C. Donald, R. J. Dowdall, B. Galloway, P. Knecht et al., *High-precision quark masses and QCD coupling from  $n_f = 4$  lattice QCD*, *Phys.Rev.* **D91** (2015) 054508, [[1408.4169](#)].
- [12] [RBC/UKQCD 14B] T. Blum et al., *Domain wall QCD with physical quark masses*, *Phys. Rev.* **D93** (2016) 074505, [[1411.7017](#)].
- [13] M. Gell-Mann, R. J. Oakes and B. Renner, *Behavior of current divergences under  $SU(3) \times SU(3)$* , *Phys. Rev.* **175** (1968) 2195–2199.
- [14] B. Bloch-Devaux, *Results from NA48/2 on  $\pi\pi$  scattering lengths measurements in  $K^\pm \rightarrow \pi^+\pi^-e^\pm\nu$  and  $K^\pm \rightarrow \pi^0\pi^0\pi^\pm$  decays*, *PoS CONFINEMENT8* (2008) 029.
- [15] J. Gasser, A. Rusetsky and I. Scimemi, *Electromagnetic corrections in hadronic processes*, *Eur. Phys. J.* **C32** (2003) 97–114, [[hep-ph/0305260](#)].

- [16] A. Rusetsky, *Isospin symmetry breaking*, *PoS CD09* (2009) 071, [[0910.5151](#)].
- [17] J. Gasser, *Theoretical progress on cusp effect and  $K_{\ell 4}$  decays*, *PoS KAON07* (2008) 033, [[0710.3048](#)].
- [18] H. Leutwyler, *Light quark masses*, *PoS CD09* (2009) 005, [[0911.1416](#)].
- [19] R. F. Dashen, *Chiral  $SU(3)\times SU(3)$  as a symmetry of the strong interactions*, *Phys. Rev.* **183** (1969) 1245–1260.
- [20] T. Blum et al., *Electromagnetic mass splittings of the low lying hadrons and quark masses from 2+1 flavor lattice QCD+QED*, *Phys. Rev.* **D82** (2010) 094508, [[1006.1311](#)].
- [21] A. Duncan, E. Eichten and H. Thacker, *Electromagnetic splittings and light quark masses in lattice QCD*, *Phys. Rev. Lett.* **76** (1996) 3894–3897, [[hep-lat/9602005](#)].
- [22] [RBC 07] T. Blum, T. Doi, M. Hayakawa, T. Izubuchi and N. Yamada, *Determination of light quark masses from the electromagnetic splitting of pseudoscalar meson masses computed with two flavors of domain wall fermions*, *Phys. Rev.* **D76** (2007) 114508, [[0708.0484](#)].
- [23] [MILC 04A] C. Aubin et al., *Results for light pseudoscalars from three-flavor simulations*, *Nucl. Phys. Proc. Suppl.* **140** (2005) 231–233, [[hep-lat/0409041](#)].
- [24] [MILC 04] C. Aubin et al., *Light pseudoscalar decay constants, quark masses and low energy constants from three-flavor lattice QCD*, *Phys. Rev.* **D70** (2004) 114501, [[hep-lat/0407028](#)].
- [25] [MILC 09] A. Bazavov et al., *Full nonperturbative QCD simulations with 2+1 flavors of improved staggered quarks*, *Rev. Mod. Phys.* **82** (2010) 1349–1417, [[0903.3598](#)].
- [26] [MILC 09A] A. Bazavov et al., *MILC results for light pseudoscalars*, *PoS CD09* (2009) 007, [[0910.2966](#)].
- [27] J. Bijnens and J. Prades, *Electromagnetic corrections for pions and kaons: masses and polarizabilities*, *Nucl. Phys.* **B490** (1997) 239–271, [[hep-ph/9610360](#)].
- [28] J. F. Donoghue and A. F. Perez, *The electromagnetic mass differences of pions and kaons*, *Phys. Rev.* **D55** (1997) 7075–7092, [[hep-ph/9611331](#)].
- [29] [MILC 08] S. Basak et al., *Electromagnetic splittings of hadrons from improved staggered quarks in full QCD*, *PoS LAT2008* (2008) 127, [[0812.4486](#)].
- [30] [MILC 12A] S. Basak et al., *Status of the MILC calculation of electromagnetic contributions to pseudoscalar masses*, *PoS LAT2012* (2012) 137, [[1210.8157](#)].
- [31] [MILC 13] S. Basak, A. Bazavov, C. Bernard, C. DeTar, E. Freeland et al., *Electromagnetic contributions to pseudoscalar masses*, *PoS CD12* (2012) 030, [[1301.7137](#)].
- [32] [MILC 14] S. Basak et al., *Finite-volume effects and the electromagnetic contributions to kaon and pion masses*, *PoS LATTICE2014* (2014) 116, [[1409.7139](#)].

- [33] [MILC 15A] S. Basak et al., *Electromagnetic effects on the light hadron spectrum*, *J. Phys. Conf. Ser.* **640** (2015) 012052, [[1510.04997](#)].
- [34] [BMW 10C] A. Portelli et al., *Electromagnetic corrections to light hadron masses*, *PoS LAT2010* (2010) 121, [[1011.4189](#)].
- [35] [BMW 12] A. Portelli, S. Dürr, Z. Fodor, J. Frison, C. Hoelbling et al., *Systematic errors in partially-quenched QCD plus QED lattice simulations*, *PoS LAT2011* (2011) 136, [[1201.2787](#)].
- [36] A. Portelli, *Inclusion of isospin breaking effects in lattice simulations*, *PoS LATTICE2014* (2015) 013, [[1505.07057](#)].
- [37] [RM123 13] G. M. de Divitiis, R. Frezzotti, V. Lubicz, G. Martinelli, R. Petronzio et al., *Leading isospin breaking effects on the lattice*, *Phys.Rev.* **D87** (2013) 114505, [[1303.4896](#)].
- [38] [QCDSF/UKQCD 15A] R. Horsley et al., *QED effects in the pseudoscalar meson sector*, *JHEP* **04** (2016) 093, [[1509.00799](#)].
- [39] R. Urech, *Virtual photons in chiral perturbation theory*, *Nucl. Phys.* **B433** (1995) 234–254, [[hep-ph/9405341](#)].
- [40] R. Baur and R. Urech, *On the corrections to Dashen’s theorem*, *Phys. Rev.* **D53** (1996) 6552–6557, [[hep-ph/9508393](#)].
- [41] R. Baur and R. Urech, *Resonance contributions to the electromagnetic low energy constants of chiral perturbation theory*, *Nucl. Phys.* **B499** (1997) 319–348, [[hep-ph/9612328](#)].
- [42] B. Moussallam, *A sum rule approach to the violation of Dashen’s theorem*, *Nucl. Phys.* **B504** (1997) 381–414, [[hep-ph/9701400](#)].
- [43] L. Lellouch, *Light quarks and lattice QCD, plenary talk given at Quark Confinement and the Hadron Spectrum X, 8-12 October 2012*, <http://www.confex.de>.
- [44] [FLAG 10] G. Colangelo, S. Dürr, A. Jüttner, L. Lellouch, H. Leutwyler et al., *Review of lattice results concerning low energy particle physics*, *Eur.Phys.J.* **C71** (2011) 1695, [[1011.4408](#)].
- [45] W. N. Cottingham, *The neutron proton mass difference and electron scattering experiments*, *Ann. of Phys.* **25** (1963) 424.
- [46] R. H. Socolow, *Departures from the Eightfold Way. 3. Pseudoscalar-meson electromagnetic masses*, *Phys. Rev.* **137** (1965) B1221–B1228.
- [47] D. J. Gross, S. B. Treiman and F. Wilczek, *Light quark masses and isospin violation*, *Phys. Rev.* **D19** (1979) 2188.
- [48] J. Gasser and H. Leutwyler, *Quark masses*, *Phys. Rept.* **87** (1982) 77–169.
- [49] T. Das, G. S. Guralnik, V. S. Mathur, F. E. Low and J. E. Young, *Electromagnetic mass difference of pions*, *Phys. Rev. Lett.* **18** (1967) 759–761.

- [50] J. Gasser and H. Leutwyler, *Chiral perturbation theory: expansions in the mass of the strange quark*, *Nucl. Phys.* **B250** (1985) 465.
- [51] G. Amoros, J. Bijnens and P. Talavera, *QCD isospin breaking in meson masses, decay constants and quark mass ratios*, *Nucl. Phys.* **B602** (2001) 87–108, [[hep-ph/0101127](#)].
- [52] J. Gasser and H. Leutwyler, *Chiral perturbation theory to one loop*, *Ann. Phys.* **158** (1984) 142.
- [53] [ALPHA 12] P. Fritzsch, F. Knechtli, B. Leder, M. Marinkovic, S. Schaefer et al., *The strange quark mass and the  $\Lambda$  parameter of two flavor QCD*, *Nucl.Phys.* **B865** (2012) 397–429, [[1205.5380](#)].
- [54] [ETM 10B] B. Blossier et al., *Average up/down, strange and charm quark masses with  $N_f = 2$  twisted mass lattice QCD*, *Phys. Rev.* **D82** (2010) 114513, [[1010.3659](#)].
- [55] S. Dürr and G. Koutsou, *The ratio  $m_c/m_s$  with Wilson fermions*, *Phys.Rev.Lett.* **108** (2012) 122003, [[1108.1650](#)].
- [56] [ETM 07] B. Blossier et al., *Light quark masses and pseudoscalar decay constants from  $N_f = 2$  lattice QCD with twisted mass fermions*, *JHEP* **04** (2008) 020, [[0709.4574](#)].
- [57] [CP-PACS 01] A. Ali Khan et al., *Light hadron spectroscopy with two flavors of dynamical quarks on the lattice*, *Phys. Rev.* **D65** (2002) 054505, [[hep-lat/0105015](#)].
- [58] [ALPHA 05] M. Della Morte et al., *Non-perturbative quark mass renormalization in two-flavor QCD*, *Nucl. Phys.* **B729** (2005) 117–134, [[hep-lat/0507035](#)].
- [59] R. Sommer, *A new way to set the energy scale in lattice gauge theories and its applications to the static force and  $\alpha_s$  in  $SU(2)$  Yang-Mills theory*, *Nucl. Phys.* **B411** (1994) 839–854, [[hep-lat/9310022](#)].
- [60] [QCDSF/UKQCD 04] M. Göckeler et al., *Determination of light and strange quark masses from full lattice QCD*, *Phys. Lett.* **B639** (2006) 307–311, [[hep-ph/0409312](#)].
- [61] [JLQCD/TWQCD 08A] J. Noaki et al., *Convergence of the chiral expansion in two-flavor lattice QCD*, *Phys. Rev. Lett.* **101** (2008) 202004, [[0806.0894](#)].
- [62] [QCDSF/UKQCD 06] M. Göckeler et al., *Estimating the unquenched strange quark mass from the lattice axial Ward identity*, *Phys. Rev.* **D73** (2006) 054508, [[hep-lat/0601004](#)].
- [63] [SPQcdR 05] D. Bećirević et al., *Non-perturbatively renormalised light quark masses from a lattice simulation with  $N_f = 2$* , *Nucl. Phys.* **B734** (2006) 138–155, [[hep-lat/0510014](#)].
- [64] [JLQCD 02] S. Aoki et al., *Light hadron spectroscopy with two flavors of  $O(a)$ -improved dynamical quarks*, *Phys. Rev.* **D68** (2003) 054502, [[hep-lat/0212039](#)].
- [65] [ETM 10C] M. Constantinou et al., *Non-perturbative renormalization of quark bilinear operators with  $N_f = 2$  ( $tmQCD$ ) Wilson fermions and the tree-level improved gauge action*, *JHEP* **08** (2010) 068, [[1004.1115](#)].

- [66] [HPQCD 10] C. McNeile, C. T. H. Davies, E. Follana, K. Hornbostel and G. P. Lepage, *High-precision  $c$  and  $b$  masses and QCD coupling from current-current correlators in lattice and continuum QCD*, *Phys. Rev.* **D82** (2010) 034512, [[1004.4285](#)].
- [67] [PACS-CS 12] S. Aoki, K.-I. Ishikawa, N. Ishizuka, K. Kanaya, Y. Kuramashi et al., *1+1+1 flavor QCD + QED simulation at the physical point*, *Phys.Rev.* **D86** (2012) 034507, [[1205.2961](#)].
- [68] J. Laiho and R. S. Van de Water, *Pseudoscalar decay constants, light-quark masses and  $B_K$  from mixed-action lattice QCD*, *PoS LATTICE2011* (2011) 293, [[1112.4861](#)].
- [69] [MILC 10A] A. Bazavov et al., *Staggered chiral perturbation theory in the two-flavor case and  $SU(2)$  analysis of the MILC data*, *PoS LAT2010* (2010) 083, [[1011.1792](#)].
- [70] [RBC/UKQCD 10A] Y. Aoki et al., *Continuum limit physics from 2+1 flavor domain wall QCD*, *Phys.Rev.* **D83** (2011) 074508, [[1011.0892](#)].
- [71] [HPQCD 09A] C. T. H. Davies et al., *Precise charm to strange mass ratio and light quark masses from full lattice QCD*, *Phys. Rev. Lett.* **104** (2010) 132003, [[0910.3102](#)].
- [72] [RBC/UKQCD 08] C. Allton et al., *Physical results from 2+1 flavor domain wall QCD and  $SU(2)$  chiral perturbation theory*, *Phys. Rev.* **D78** (2008) 114509, [[0804.0473](#)].
- [73] [CP-PACS/JLQCD 07] T. Ishikawa et al., *Light quark masses from unquenched lattice QCD*, *Phys. Rev.* **D78** (2008) 011502, [[0704.1937](#)].
- [74] [HPQCD 05] Q. Mason, H. D. Trottier, R. Horgan, C. T. H. Davies and G. P. Lepage, *High-precision determination of the light-quark masses from realistic lattice QCD*, *Phys. Rev.* **D73** (2006) 114501, [[hep-ph/0511160](#)].
- [75] [HPQCD/MILC/UKQCD 04] C. Aubin et al., *First determination of the strange and light quark masses from full lattice QCD*, *Phys. Rev.* **D70** (2004) 031504, [[hep-lat/0405022](#)].
- [76] T. van Ritbergen, J. A. M. Vermaseren and S. A. Larin, *The four-loop  $\beta$ -function in Quantum Chromodynamics*, *Phys. Lett.* **B400** (1997) 379–384, [[hep-ph/9701390](#)].
- [77] K. G. Chetyrkin and A. Retey, *Renormalization and running of quark mass and field in the regularization invariant and  $\overline{MS}$  schemes at three and four loops*, *Nucl. Phys.* **B583** (2000) 3–34, [[hep-ph/9910332](#)].
- [78] PARTICLE DATA GROUP collaboration, K. A. Olive et al., *Review of Particle Physics*, *Chin. Phys.* **C38** (2014) 090001 and 2015 update.
- [79] [HPQCD 08B] I. Allison et al., *High-precision charm-quark mass from current-current correlators in lattice and continuum QCD*, *Phys. Rev.* **D78** (2008) 054513, [[0805.2999](#)].
- [80] M. Lüscher, R. Narayanan, P. Weisz and U. Wolff, *The Schrödinger functional: a renormalizable probe for non-abelian gauge theories*, *Nucl. Phys.* **B384** (1992) 168–228, [[hep-lat/9207009](#)].

- [81] C. A. Dominguez, N. F. Nasrallah, R. Röntsch and K. Schilcher, *Light quark masses from QCD sum rules with minimal hadronic bias*, *Nucl. Phys. Proc. Suppl.* **186** (2009) 133–136, [[0808.3909](#)].
- [82] K. G. Chetyrkin and A. Khodjamirian, *Strange quark mass from pseudoscalar sum rule with  $O(\alpha_s^4)$  accuracy*, *Eur. Phys. J.* **C46** (2006) 721–728, [[hep-ph/0512295](#)].
- [83] M. Jamin, J. A. Oller and A. Pich, *Scalar  $K\pi$  form factor and light quark masses*, *Phys. Rev.* **D74** (2006) 074009, [[hep-ph/0605095](#)].
- [84] S. Narison, *Strange quark mass from  $e^+e^-$  revisited and present status of light quark masses*, *Phys. Rev.* **D74** (2006) 034013, [[hep-ph/0510108](#)].
- [85] A. I. Vainshtein et al., *Sum rules for light quarks in Quantum Chromodynamics*, *Sov. J. Nucl. Phys.* **27** (1978) 274.
- [86] K. Maltman and J. Kambor,  *$m_u + m_d$  from isovector pseudoscalar sum rules*, *Phys. Lett.* **B517** (2001) 332–338, [[hep-ph/0107060](#)].
- [87] [ETM 14D] A. Abdel-Rehim, C. Alexandrou, P. Dimopoulos, R. Frezzotti, K. Jansen et al., *Progress in Simulations with Twisted Mass Fermions at the Physical Point*, *PoS LATTICE2014* (2014) 119, [[1411.6842](#)].
- [88] S. Weinberg, *The problem of mass*, *Trans. New York Acad. Sci.* **38** (1977) 185–201.
- [89] J. A. Oller and L. Roca, *Non-perturbative study of the light pseudoscalar masses in chiral dynamics*, *Eur. Phys. J.* **A34** (2007) 371–386, [[hep-ph/0608290](#)].
- [90] R. Kaiser, *The  $\eta$  and the  $\eta'$  at large  $N_c$ , diploma work*, University of Bern (1997); H. Leutwyler, *On the  $1/N$ -expansion in chiral perturbation theory*, *Nucl. Phys. Proc. Suppl.* **64** (1998) 223–231, [[hep-ph/9709408](#)].
- [91] H. Leutwyler, *The ratios of the light quark masses*, *Phys. Lett.* **B378** (1996) 313–318, [[hep-ph/9602366](#)].
- [92] [QCDSF/UKQCD 15] R. Horsley et al., *Isospin splittings of meson and baryon masses from three-flavor lattice QCD + QED*, *J. Phys.* **G43** (2016) 10LT02, [[1508.06401](#)].
- [93] [RM123 11] G. M. de Divitiis, P. Dimopoulos, R. Frezzotti, V. Lubicz, G. Martinelli et al., *Isospin breaking effects due to the up-down mass difference in lattice QCD*, *JHEP* **1204** (2012) 124, [[1110.6294](#)].
- [94] J. Gasser and H. Leutwyler,  *$\eta \rightarrow 3\pi$  to one loop*, *Nucl. Phys.* **B250** (1985) 539.
- [95] J. Kambor, C. Wiesendanger and D. Wyler, *Final state interactions and Khuri-Treiman equations in  $\eta \rightarrow 3\pi$  decays*, *Nucl. Phys.* **B465** (1996) 215–266, [[hep-ph/9509374](#)].
- [96] A. V. Anisovich and H. Leutwyler, *Dispersive analysis of the decay  $\eta \rightarrow 3\pi$* , *Phys. Lett.* **B375** (1996) 335–342, [[hep-ph/9601237](#)].
- [97] C. Ditsche, B. Kubis and U.-G. Meißner, *Electromagnetic corrections in  $\eta \rightarrow 3\pi$  decays*, *Eur. Phys. J.* **C60** (2009) 83–105, [[0812.0344](#)].



- [98] G. Colangelo, S. Lanz and E. Passemar, *A new dispersive analysis of  $\eta \rightarrow 3\pi$* , *PoS CD09* (2009) 047, [[0910.0765](#)].
- [99] J. Bijnens and K. Ghorbani,  *$\eta \rightarrow 3\pi$  at two loops in chiral perturbation theory*, *JHEP* **11** (2007) 030, [[0709.0230](#)].
- [100] [JLQCD 15B] K. Nakayama, B. Fahy and S. Hashimoto, *Charmonium current-current correlators with Mobius domain-wall fermion*, in *Proceedings, 33rd International Symposium on Lattice Field Theory (Lattice 2015)*, vol. LATTICE2015, p. 267, 2016. [1511.09163](#).
- [101] [ETM 11F] K. Jansen, M. Petschlies and C. Urbach, *Charm Current-Current Correlators in Twisted Mass Lattice QCD*, *PoS LATTICE2011* (2011) 234, [[1111.5252](#)].
- [102] [ETM 14A] C. Alexandrou, V. Drach, K. Jansen, C. Kallidonis and G. Koutsou, *Baryon spectrum with  $N_f = 2 + 1 + 1$  twisted mass fermions*, *Phys. Rev.* **D90** (2014) 074501, [[1406.4310](#)].
- [103] [ $\chi$ QCD 14] Y. Yi-Bo et al., *Charm and strange quark masses and  $f_{D_s}$  from overlap fermions*, *Phys. Rev.* **D92** (2015) 034517, [[1410.3343](#)].
- [104] [ALPHA 13B] J. Heitger, G. M. von Hippel, S. Schaefer and F. Virotta, *Charm quark mass and  $D$ -meson decay constants from two-flavour lattice QCD*, *PoS LATTICE2013* (2014) 475, [[1312.7693](#)].
- [105] [QCDSF 10] W. Bietenholz et al., *Pion in a box*, *Phys. Lett.* **B687** (2010) 410–414, [[1002.1696](#)].
- [106] S. Dürr and G. Koutsou, *Brillouin improvement for Wilson fermions*, *Phys. Rev.* **D83** (2011) 114512, [[1012.3615](#)].
- [107] [HPQCD 14B] B. Colquhoun, R. J. Dowdall, C. T. H. Davies, K. Hornbostel and G. P. Lepage,  *$\Upsilon$  and  $\Upsilon'$  Leptonic Widths,  $a_\mu^b$  and  $m_b$  from full lattice QCD*, *Phys. Rev.* **D91** (2015) 074514, [[1408.5768](#)].
- [108] [ETM 14B] A. Bussone et al., *Heavy flavour precision physics from  $N_f = 2 + 1 + 1$  lattice simulations*, in *International Conference on High Energy Physics 2014 (ICHEP 2014) Valencia, Spain, July 2-9, 2014*, vol. 273-275, pp. 273–275, 2016. [1411.0484](#). DOI.
- [109] [HPQCD 13B] A.J. Lee et al., *Mass of the  $b$  quark from lattice NRQCD and lattice perturbation theory*, *Phys. Rev.* **D87** (2013) 074018, [[1302.3739](#)].
- [110] [ETM 13B] N. Carrasco et al.,  *$B$ -physics from  $N_f = 2$  tmQCD: the Standard Model and beyond*, *JHEP* **1403** (2014) 016, [[1308.1851](#)].
- [111] [ALPHA 13C] F. Bernardoni et al., *The  $b$ -quark mass from non-perturbative  $N_f = 2$  Heavy Quark Effective Theory at  $O(1/m_h)$* , *Phys. Lett.* **B730** (2014) 171–177, [[1311.5498](#)].
- [112] [ETM 11A] P. Dimopoulos et al., *Lattice QCD determination of  $m_b$ ,  $f_B$  and  $f_{B_s}$  with twisted mass Wilson fermions*, *JHEP* **1201** (2012) 046, [[1107.1441](#)].